

Joint Beamforming and Power Allocation for RIS Aided Full-Duplex Integrated Sensing and Uplink Communication System

Yuan Guo, Yang Liu, Qingqing Wu, Xiaoyang Li, and Qingjiang Shi

Abstract—Integrated sensing and communication (ISAC) capability is envisioned as one key feature for future cellular networks. Classical half-duplex (HD) radar sensing is conducted in a “first-emit-then-listen” manner. One challenge to realize HD ISAC lies in the discrepancy of the two systems’ time scheduling for transmitting and receiving. This difficulty can be overcome by full-duplex (FD) transceivers. Besides, ISAC generally has to compromise its communication rate due to realizing sensing functionality. This loss can be compensated by the emerging reconfigurable intelligent surface (RIS) technology. This paper considers the joint design of beamforming, power allocation and signal processing in a FD uplink communication system aided by RIS, which is a highly nonconvex problem. To resolve this challenge, via leveraging the cutting-the-edge majorization-minimization (MM) and penalty-dual-decomposition (PDD) methods, we develop an iterative solution that optimizes all variables via using convex optimization techniques. Besides, by wisely exploiting alternative direction method of multipliers (ADMM) and optimality analysis, we further develop a low complexity solution that updates all variables analytically and runs highly efficiently. Numerical results are provided to verify the effectiveness and efficiency of our proposed algorithms and demonstrate the significant performance boosting by employing RIS in the FD ISAC system.

Index Terms—integrated sensing and communication (ISAC), reconfigurable intelligent surface (RIS), full-duplex (FD), low-complexity algorithm.

I. INTRODUCTION

Recently, the integrated sensing and communication (ISAC) system has attracted great attentions from both industry and academia [1]–[3]. On the one hand, next generation cellular system featured by millimeter wave (mmWave) and Terahertz communication techniques will occupy wide high-frequency bands, which overlap with those for radar systems. On the other hand, the booming Internet of Things (IoT) applications require mobile devices to become more functional and possess sensing capability. In this context, ISAC has been envisioned as a promising solution, which aims at realizing both sensing and communication functionalities using one unified hardware set and sharing frequency spectrums. Many latest progresses

for joint radar sensing and communication design can be found in [1]–[3] and the reference therein.

Despite its hardware and spectral efficiency, the ISAC system’s dual functionalities generally come at a cost of compromising performance in both sensing and communication. This drawback can hopefully be overcome by the emerging reconfigurable intelligent surface (RIS) technology [4], which is also widely known as intelligent reflecting surface (IRS) [5]. The RIS is envisioned as a viable approach to enhance communication system. It can empower the wireless system with additional beamforming capability via reflecting and adjusting phase shifts of the incoming signals at a relatively low energy and hardware expense. The versatility of RIS in boosting communication performance in various aspects have been extensively verified recently, see [4] and [5] and their reference.

A. Related Works

Due to the aforementioned advantage of the ISAC system and the merits of RIS technology, a rich body of literature has studied deploying the RIS in ISAC context and conducted joint design to improve the sensing and communication performance, e.g., [6]–[25]. For instance, the authors of [6] and [7] first proposed to leverage RIS in ISAC system and demonstrated that RIS could effectively reduce multi-user interference (MUI) and Cramér-Rao bound (CRB) of the radar sensing signal, respectively. The work [8] showed that, via deploying RIS, joint active and passive beamforming design could significantly improve the signal-to-noise-ratio (SNR) of radar signal processing while guaranteeing the quality-of-service (QoS) of mobile users. The authors of [10] proposed a RIS-aided waveform design towards maximizing the weighted sum of radar sensing SNR and information receiving SNR, which was shown to boost both functionals. The works [11] utilized RIS to improve communication performance under the cross-correlation constraint. The authors of [12] considered sensing target with non-negligible shape and illustrated that RIS could greatly enhance the ultimate detection resolution (UDR) of target detection. The authors of [13] developed a low-complexity RIS beamforming algorithm which could maximize both the communication and sensing SNR. The paper [14] showed that RIS could effectively elevate the radar mutual information (MI), which is generally a good performance metric for both detection and estimation. The recent works [15]–[16] employed the novel simultaneously

Y. Guo and Y. Liu are with the School of Information and Communication Engineering, Dalian University of Technology, Dalian, China, email: yuan-guo@mail.dlut.edu.cn, yangliu_613@dlut.edu.cn.

Q. Wu is with Department of Electronic Engineering, Shanghai Jiao Tong University, Shanghai, China, email: qingqingwu@sjtu.edu.cn.

X. Li is with the Shenzhen Research Institute of Big Data, Shenzhen, China, email: lixiaoyang@sribd.cn.

Q. Shi is with the School of Software Engineering, Tongji University, Shanghai, China, and also with the Shenzhen Research Institute of Big Data, Shenzhen, China, email: shiq@tongji.edu.cn.

transmitting and reflecting (STAR) architecture to effectively extend the RIS' coverage in ISAC network. Lately, the authors of [17] adopted the emerging active RIS architecture in ISAC system and showed it could significantly boost signal-to-interference-plus-noise-ratio (SINR) of radar sensing compared to the passive RIS. The papers [18]–[19] demonstrated that RIS could remarkably enhance the security of sensing when the probing signal contained communication information. The recent work [20] proposed four different algorithms to enhance the RIS-aided ISAC system's performance. The works [21] and [22] demonstrated that the deployment of RIS could remarkably inflate the beam pattern gain in non-orthogonal multiple access (NOMA) and millimeter wave ISAC networks, respectively. Besides, very recently, several latest works paid attention to implementing ISAC systems utilizing full-duplex (FD) BSs [23]–[25]. The authors of [23] optimized FD BS' hybrid precoder to enhance mobile users' spectral efficiency and radar sensing capability. The work [24] designed FD ISAC system's waveform to improve radar detection probability via suppressing self-interference and enhancing autocorrelation. In [25], the authors developed secure communication beamforming aided by RIS in a uplink communication system with FD BS

B. Motivations and Contributions

As seen above, although a rich body of existing literature has investigated the waveform design for ISAC system, most of these works have considered half-duplex (HD) systems, where transmitting and receiving (T&R) are operated separately in time. Note the switching frequencies between T&R are usually different for communication and radar sensing, which is indeed one challenge to implement ISAC system [3]. For instance, the 3GPP NR specification [26] has supported flexible UL/DL mini-slot frame structures, which will inevitably lead to more unpredictable T&R switching frequency for communication. In contrast, the FD system tends to be a highly promising solution to accommodate the aforementioned conflict [2]–[3]. Note the waveform design in FD ISAC system has far from being thoroughly investigated, except the small number of latest works [23]–[25]. More importantly, all the existing works [23]–[25] have not considered the deployment of RIS in the FD system. Based on the above inspections, we are motivated to study a RIS-aided FD ISAC system to fully promote its communication and sensing capabilities. Specifically, the contributions of this paper are elaborated as follows:

- This paper considers the joint beamforming design in a FD ISAC system aided by RIS to realize simultaneous UL communication and target sensing. We study maximizing the sum-rate of all UL users while assuring the radar sensing quality via designing BS probing beamforming, RIS phase-shifts, users power allocation and receiving processors. To the best of our knowledge, this problem has not been considered in the existing literature, e.g., [6]–[25].
- Moreover, this paper considers a very generic signal propagation model, which fully takes into account the RIS

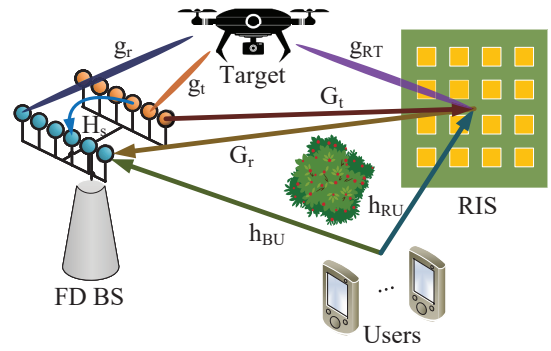


Fig. 1. An RIS-aided FD ISAC system.

effect in both the forwarding and reflected radar probing signals. As will be seen, this consideration in modeling significantly complicates the beamforming design task and yields a highly challenging quartic fractional programming problem.

- To attack the above challenge, we develop an alternative optimization algorithm that optimizes all variables via convex optimization techniques. Especially, to tackle the highly challenging RIS configuration problem, by wisely introducing splitting variable and leveraging the penalty dual decomposition (PDD) [27] framework combined with the majorization-minimization (MM) [28] method, we obtain a solution to resolve the quartic optimization by solving a series of quadratic sub-problems. This method is never seen in the existing literature.
- Furthermore, we also develop low complexity solution. By exploiting alternative direction method of multipliers (ADMM) [29] and analyzing optimality conditions, we succeed in optimizing all blocks of variables analytically. Our proposed analytic-updated solution does not resort to any numerical solver, e.g., CVX [30], and is rarely seen in the existing literature, e.g., [6]–[25].
- Last but not least, extensive numerical results are provided to verify the effectiveness and efficiency of our proposed solutions. At the same time, experiment results demonstrate that the deployment of RIS can significantly benefit the UL communication in the considered FD ISAC scenario.

The rest of the paper is organized as follows. Section II will introduce the model of a FD ISAC system assisted by RIS and formulate the joint beamforming design problem. Section III will propose an iterative solution to tackle the proposed beamforming design problem. A low complexity algorithm will be developed in Section IV. Section V and Section VI will present numerical results and conclude the paper, respectively.

II. SYSTEM MODEL AND PROBLEM FORMULATION

A. System Model

As shown in Fig. 1, we consider an uplink multi-user MISO RIS-aided ISAC system consisting a FD BS equipped with N_t transmit (TX) antennas and N_r receiver (RX) antennas, an RIS with M reflecting units, K single-antenna uplink

mobile users and one point-like target¹. The BS with aid of an RIS simultaneously receives the information from mobile users and transmits probing waveform to detect the target. For convenience, the sets of users and RIS units are denoted by $\mathcal{K} = \{1, \dots, K\}$ and $\mathcal{M} = \{1, \dots, M\}$, respectively. Besides, we assume that the transmission links between target and users are blocked.

The uplink signal transmitted by the k -th uplink mobile user can be written as

$$x_{u,k} = \sqrt{q_k} s_{u,k}, \forall k \in \mathcal{K}, \quad (1)$$

where $\mathcal{K} \triangleq \{1, \dots, K\}$, $s_{u,k}$ and q_k are the information symbol and transmission power of k -th user, respectively. For simplicity, we assume that $s_{u,k}$ are mutually uncorrelated and each has zero mean and unit variance.

To conduct target sensing, the BS transmits probing signal, which is given as [31]-[32]

$$\mathbf{x} = \mathbf{W} \mathbf{s}_r, \quad (2)$$

where the vector $\mathbf{s}_r \in \mathbb{C}^{N_t \times 1}$ denotes radar probing signal and has zero mean and covariance matrix $\mathbb{E}\{\mathbf{s}_r \mathbf{s}_r^H\} = \mathbf{I}_{N_t}$, and $\mathbf{W} \in \mathbb{C}^{N_t \times N_t}$ represents the beamformer for the probing signal.

As shown in Fig. 1, we denote the wireless links of BS TX-RIS, BS RX-RIS, BS TX-user- k , RIS-user- k , RIS-target and the self-interference (SI) of the BS as $\mathbf{G}_t \in \mathbb{C}^{M \times N_t}$, $\mathbf{G}_r \in \mathbb{C}^{M \times N_r}$, $\mathbf{h}_{BU,k} \in \mathbb{C}^{N_r \times 1}$, $\mathbf{h}_{RU,k} \in \mathbb{C}^{M \times 1}$, $\mathbf{g}_{RT} \in \mathbb{C}^{M \times 1}$ and $\mathbf{H}_s \in \mathbb{C}^{N_t \times N_r}$, respectively. The phase-shifting conducted by the RIS elements to their impinging signals can be modeled as a complex vector $\boldsymbol{\phi} = [e^{j\theta_1}, \dots, e^{j\theta_M}]^T$, with θ_m representing the phase shift of m -th reflecting unit, $\theta_m \in [0, 2\pi)$ and $\forall m \in \mathcal{M}$. In the following, we will alternatively use the diagonal matrix $\boldsymbol{\Phi} \triangleq \text{diag}(\boldsymbol{\phi})$ to represent the RIS' reflection coefficients.

The steering vectors of BS can be expressed as

$$\mathbf{a}_t = [1, e^{-j2\pi d \sin(\theta_t)/\lambda}, \dots, e^{-j2\pi d(N_t-1) \sin(\theta_t)/\lambda}]^T \in \mathbb{C}^{N_t \times 1}, \quad (3a)$$

$$\mathbf{a}_r = [1, e^{-j2\pi d \sin(\theta_r)/\lambda}, \dots, e^{-j2\pi d(N_r-1) \sin(\theta_r)/\lambda}]^T \in \mathbb{C}^{N_r \times 1}, \quad (3b)$$

respectively, where d denoting the antenna spacing and λ denoting the carrier wavelength. θ_t and θ_r are the angle of departure (AoD) and angle of arrival (AoA) with respect to transmit and receive antennas of the BS, respectively.

The steering vector of RIS is expressed as

$$\mathbf{a}_{RT}(\mathbf{g}_R) = \mathbf{a}_{M_1}(g_{R,1}) \otimes \mathbf{a}_{M_2}(g_{R,2}), \quad (4)$$

with

$$\mathbf{g}_R = \{g_{R,1} = \frac{1}{2} \sin(\theta_{R,e}) \cos(\theta_{R,z}), g_{R,2} = \frac{1}{2} \cos(\theta_{R,e})\}, \quad (5a)$$

$$\mathbf{a}_{M_1}(g_{R,1}) = [1, e^{j2\pi d g_{R,1}/\lambda}, \dots, e^{j2\pi d(M_1-1) g_{R,1}/\lambda}]^T \in \mathbb{C}^{M_1 \times 1}, \quad (5b)$$

$$\mathbf{a}_{M_2}(g_{R,2}) = [1, e^{j2\pi d g_{R,2}/\lambda}, \dots, e^{j2\pi d(M_2-1) g_{R,2}/\lambda}]^T \in \mathbb{C}^{M_2 \times 1}, \quad (5c)$$

where $\theta_{R,e}$ and $\theta_{R,z}$ represent elevation and azimuth angles of the angle of departure (AoD) of the RIS, respectively. Besides, M_1 and M_2 denote the numbers of elevation and azimuth RIS'

¹In fact, the solution developed in this paper can be easily extended to the multi-target scheme. Due to space of limit, we leave the multi-target case for future study.

elements, respectively, and the total number of RIS' elements is $M = M_1 \times M_2$.

Therefore, the BS TX-target, the BS RX-target and RIS-target channels are given as

$$\mathbf{g}_t = \alpha_t \mathbf{a}_t \in \mathbb{C}^{N_t \times 1}, \mathbf{g}_r = \alpha_r \mathbf{a}_r \in \mathbb{C}^{N_r \times 1}, \mathbf{g}_{RT} = \alpha_{RT} \mathbf{a}_{RT} \in \mathbb{C}^{M \times 1}, \quad (6)$$

respectively, where α_t , α_r and α_{RT} are complex fading coefficients and are assumed to be known.

To perform target sensing, the BS emits probing waveform towards the target and listens to its echoes rebounding from the target simultaneously. During the whole procedure, all mobile users are operating in uplink mode and transmitting information symbols to the BS. The received signal at FD BS can be represented by

$$\mathbf{y} = \underbrace{\sum_{k=1}^K (\mathbf{h}_{BU,k} + \mathbf{G}_r^H \boldsymbol{\Phi} \mathbf{h}_{RU,k}) x_{u,k}}_{\text{UL communication signal}} + \underbrace{(\mathbf{G}_r^H \boldsymbol{\Phi} \mathbf{G}_t + \mathbf{H}_s^H) \mathbf{x}}_{\text{self-interference}} + \underbrace{\alpha (\mathbf{g}_r + \mathbf{G}_r^H \boldsymbol{\Phi} \mathbf{g}_{RT}) (\mathbf{g}_t^H + \mathbf{g}_{RT}^T \boldsymbol{\Phi} \mathbf{G}_t) \mathbf{x}}_{\text{sensing echoes}} + \mathbf{n}_{BS}, \quad (7)$$

where α denotes the target radar cross section (RCS) and $\mathbb{E}\{|\alpha|^2\} = \sigma_t^2$, $\mathbf{n}_{BS} \sim \mathcal{CN}(0, \mathbf{I}_{N_r})$ is the complex additive white Gaussian noise (AWGN) at the BS. Note in (7), the signals reflected more than thrice are neglected due to the severe attenuations.

To recover different users' information and improve target sensing performance, the BS utilizes $K+1$ linear filters $\mathbf{u}_j \in \mathbb{C}^{N_r \times 1}$, $\forall j \in \mathcal{J} \triangleq \{0\} \cup \mathcal{K}$ to post-process the received signal, where index 0 corresponds to the radar sensing filter bank. Therefore, the output of the j -th post-processor is given as

$$y_j = \mathbf{u}_j^H \mathbf{y}, \forall j \in \mathcal{J}. \quad (8)$$

The SINR for the k -th mobile user can be readily obtained as

$$\text{SINR}_{U,k}(\mathbf{W}, \mathbf{u}_k, \{q_k\}, \boldsymbol{\phi}) = \quad (9)$$

$$\frac{q_k |\mathbf{u}_k^H \mathbf{h}_{U,k}|^2}{\sum_{i \neq k} q_i |\mathbf{u}_k^H \mathbf{h}_{U,i}|^2 + \sigma_t^2 \|\mathbf{u}_k^H \mathbf{H}(\boldsymbol{\Phi}) \mathbf{W}\|_2^2 + \|\mathbf{u}_k^H \mathbf{G} \mathbf{W}\|_2^2 + \sigma_r^2 \|\mathbf{u}_k^H\|_2^2},$$

where $\mathbf{h}_{U,k} \triangleq \mathbf{h}_{BU,k} + \mathbf{G}_r^H \boldsymbol{\Phi} \mathbf{h}_{RU,k}$, $\mathbf{G} \triangleq \mathbf{G}_r^H \boldsymbol{\Phi} \mathbf{G}_t + \mathbf{H}_s^H$ and $\mathbf{H}(\boldsymbol{\Phi}) \triangleq (\mathbf{g}_r + \mathbf{G}_r^H \boldsymbol{\Phi} \mathbf{g}_{RT})(\mathbf{g}_t^H + \mathbf{g}_{RT}^T \boldsymbol{\Phi} \mathbf{G}_t)$.

The achievable rate of each user is given as

$$R_k(\mathbf{W}, \mathbf{u}_k, \{q_k\}, \boldsymbol{\phi}) = \log(1 + \text{SINR}_{U,k}), \forall k \in \mathcal{K}. \quad (10)$$

The output SINR for target sensing can be given by

$$\text{SINR}_r(\mathbf{W}, \mathbf{u}_0, \{q_k\}, \boldsymbol{\phi}) = \quad (11)$$

$$\frac{\sigma_t^2 \|\mathbf{u}_0^H \mathbf{H}(\boldsymbol{\Phi}) \mathbf{W}\|_2^2}{\sum_{k=1}^K q_k |\mathbf{u}_0^H \mathbf{h}_{U,k}|^2 + \|\mathbf{u}_0^H \mathbf{G} \mathbf{W}\|_2^2 + \sigma_r^2 \|\mathbf{u}_0^H\|_2^2}.$$

B. Problem Formulation

Our goal is to maximize the sum-rate of all users via jointly optimizing the transmit beamformer \mathbf{W} , the linear post-processing filters ($\{\mathbf{u}_k\}, \mathbf{u}_0$), the users' uplink transmit power $\{q_k\}$ and the reflected phase shift $\boldsymbol{\phi}$. The optimization problem can be formulated as

$$(P0) : \max_{\mathbf{W}, \{\mathbf{u}_k\}, \mathbf{u}_0, \{q_k\}, \boldsymbol{\phi}} \sum_{k=1}^K R_k(\mathbf{W}, \mathbf{u}_k, \{q_k\}, \boldsymbol{\phi}) \quad (12a)$$

$$\begin{aligned}
 & \mathbf{R}_k(\mathbf{W}, \mathbf{u}_k, \{q_k\}, \phi) \\
 &= \max_{\omega_k \geq 0} \log(\omega_k) - \omega_k \left(\sum_{i=1}^K q_i |\mathbf{u}_k^H \mathbf{h}_{U,k}|^2 + \sigma_t^2 \|\mathbf{u}_k^H \mathbf{H}(\Phi) \mathbf{W}\|_2^2 + \|\mathbf{u}_k^H \mathbf{G} \mathbf{W}\|_2^2 + \sigma_r^2 \|\mathbf{u}_k^H\|_2^2 \right)^{-1} \sqrt{q_k} \mathbf{u}_k^H \mathbf{h}_{U,k} + 1 \\
 &= \max_{\omega_k \geq 0, \beta_k} \underbrace{\log(\omega_k) - \omega_k \left(1 - 2\text{Re}\{\beta_k^* \sqrt{q_k} \mathbf{u}_k^H \mathbf{h}_{U,k}\} + |\beta_k|^2 \left(\sum_{i=1}^K q_i |\mathbf{u}_k^H \mathbf{h}_{U,k}|^2 + \sigma_t^2 \|\mathbf{u}_k^H \mathbf{H}(\Phi) \mathbf{W}\|_2^2 + \|\mathbf{u}_k^H \mathbf{G} \mathbf{W}\|_2^2 + \sigma_r^2 \|\mathbf{u}_k^H\|_2^2 \right) \right)}_{\tilde{\mathbf{R}}_k(\mathbf{W}, \mathbf{u}_k, \{q_k\}, \phi, \omega_k, \beta_k)} + 1, \forall k \in \mathcal{K}.
 \end{aligned}$$

$$\text{s.t. SINR}_r(\mathbf{W}, \mathbf{u}_0, \{q_k\}, \phi) \geq \Gamma_r, \quad (12b)$$

$$\|\mathbf{W}\|_F^2 \leq P_{BS}, \quad (12c)$$

$$0 \leq q_k \leq P_{U,k}, \forall k \in \mathcal{K}, \quad (12d)$$

$$|\phi_m| = 1, \forall m \in \mathcal{M}, \quad (12e)$$

where Γ_r and P_{BS} denote the predefined target sensing performance threshold and the maximum transmission power of the BS, respectively, and $P_{U,k}$ is the uplink communication power budget of k -th user. The problem (P0) is highly challenging due to its highly non-convex objective and constraints.

III. SOCP-BASED ALGORITHM

A. Problem Reformulation

In order to make the problem (P0) more tractable, we firstly employ the weighted minimum mean squared error (WMMSE) method [33] to transform its objective function. Specifically, via introducing auxiliary variables $\{\beta_k\}$ and $\{\omega_k\}$, the original objective function (12a) can be equivalently written into a variation form (13) [33], as shown on the top of next page. Therefore, the original problem (P0) is equivalently expressed as

$$(P1) : \max_{\substack{\mathbf{W}, \{\mathbf{u}_k\}, \mathbf{u}_0, \\ \{q_k\}, \phi, \{\omega_k\}, \{\beta_k\}}} \sum_{k=1}^K \tilde{\mathbf{R}}_k(\mathbf{W}, \{\mathbf{u}_k\}, \{q_k\}, \phi, \omega_k, \beta_k) \quad (14a)$$

$$\text{s.t. SINR}_r(\mathbf{W}, \mathbf{u}_0, \{q_k\}, \phi) \geq \Gamma_r, \quad (14b)$$

$$\|\mathbf{W}\|_F^2 \leq P_{BS}, \quad (14c)$$

$$0 \leq q_k \leq P_{U,k}, \forall k \in \mathcal{K}, \quad (14d)$$

$$|\phi_m| = 1, \forall m \in \mathcal{M}. \quad (14e)$$

In the next, we adopt the block coordinate ascent (BCA) [34] method to tackle the problem (P1).

B. Optimizing auxiliary variables

According to the derivation of WMMSE transformation, with other variables being fixed, the update of the auxiliary variables $\{\beta_k\}$ and $\{\omega_k\}$ have analytical solutions that are given as follows

$$\beta_k^* = \frac{\sqrt{q_k} \mathbf{u}_k^H \mathbf{h}_{U,k}}{\sum_{i=1}^K q_i |\mathbf{u}_k^H \mathbf{h}_{U,i}|^2 + \sigma_t^2 \|\mathbf{u}_k^H \mathbf{H} \mathbf{W}\|_2^2 + \|\mathbf{u}_k^H \mathbf{G} \mathbf{W}\|_2^2 + \sigma_r^2 \|\mathbf{u}_k^H\|_2^2}, \quad (15)$$

$$\omega_k^* = 1 + \frac{q_k \mathbf{u}_k^H \mathbf{h}_{U,k} \mathbf{u}_k \mathbf{u}_k^H \mathbf{h}_{U,k}}{\sum_{i \neq k} q_i |\mathbf{u}_k^H \mathbf{h}_{U,i}|^2 + \sigma_t^2 \|\mathbf{u}_k^H \mathbf{H} \mathbf{W}\|_2^2 + \|\mathbf{u}_k^H \mathbf{G} \mathbf{W}\|_2^2 + \sigma_r^2 \|\mathbf{u}_k^H\|_2^2}. \quad (16)$$

C. Optimizing The Phase Shift

In this subsection, we investigate the optimization of the RIS phase-shifting ϕ when other variables are given. By introducing the new coefficients as follows

$$\mathbf{P}_k \triangleq \mathbf{G}_r^H \text{diag}(\mathbf{h}_{RU,k}), \mathbf{r}_k \triangleq \mathbf{G}_r \mathbf{u}_k, \mathbf{v}_k \triangleq \mathbf{u}_k^H \mathbf{H}_s^H \mathbf{W}, \quad (17)$$

$$\begin{aligned}
 \mathbf{S}_k &\triangleq \mathbf{W}^H \mathbf{G}_t^H \text{diag}(\mathbf{r}_k), \mathbf{r}_0 \triangleq \mathbf{G}_r \mathbf{u}_0, \mathbf{v}_0 \triangleq \mathbf{u}_0^H \mathbf{H}_s^H \mathbf{W}, \\
 \mathbf{S}_0 &\triangleq \mathbf{W}^H \mathbf{G}_t^H \text{diag}(\mathbf{r}_0), \mathbf{a}_{1,k} \triangleq \mathbf{W}^H \mathbf{g}_t \mathbf{g}_r^H \mathbf{u}_k, \mathbf{b}_3 \triangleq \mathbf{W}^H \mathbf{g}_t, \\
 b_{1,k} &\triangleq \mathbf{g}_r^H \mathbf{u}_k, \mathbf{B} \triangleq \text{diag}(\mathbf{g}_{RT}^H) \mathbf{G}_t \mathbf{W}, b_{2,k} \triangleq \text{diag}(\mathbf{g}_{RT}^H) \mathbf{G}_r \mathbf{u}_k, \\
 \mathbf{a}_0 &\triangleq \mathbf{W}^H \mathbf{g}_t \mathbf{g}_r^H \mathbf{u}_0, b_{0,1} \triangleq \mathbf{g}_r^H \mathbf{u}_0, \mathbf{b}_{0,2} \triangleq \text{diag}(\mathbf{g}_{RT}^H) \mathbf{G}_r \mathbf{u}_0,
 \end{aligned}$$

the objective function (14a) and the constraint (14b) are, respectively, rewritten in (18a) and (18b) as follows

$$- \sum_{k=1}^K \tilde{\mathbf{R}}_k = \phi^H \mathbf{T}_1 \phi - 2\text{Re}\{\mathbf{t}_1^H \phi\} + c_1 \quad (18a)$$

$$+ 2\text{Re}\{\phi^H \mathbf{T}_{1,5} \phi^* + \text{vec}(\phi \phi^T)^H \mathbf{T}_{1,67} \phi\}$$

$$+ \text{vec}(\phi \phi^T)^H \mathbf{T}_{1,8} \text{vec}(\phi \phi^T),$$

$$\phi^H \mathbf{T}_0 \phi - 2\text{Re}\{\mathbf{t}_0^H \phi\} + c_2 - \phi^H \mathbf{T}_{0,0} \phi \quad (18b)$$

$$- 2\text{Re}\{\phi^H \mathbf{T}_{0,5} \phi^* + \text{vec}(\phi \phi^T)^H \mathbf{T}_{0,67} \phi\}$$

$$- \text{vec}(\phi \phi^T)^H \mathbf{T}_{0,8} \text{vec}(\phi \phi^T) \leq 0,$$

with the parameters in (18a) and (18b) being defined in (19), as shown on the top of next page.

Based on the above transformation, the reflection phase shift optimization reduces to solving the following problem

$$(P2) : \min_{\phi} \phi^H \mathbf{T} \phi - 2\text{Re}\{\mathbf{t}_1^H \phi\} + c_1 \quad (20a)$$

$$+ 2\text{Re}\{\phi^H \mathbf{T}_{1,5} \phi^* + \text{vec}(\phi \phi^T)^H \mathbf{T}_{1,67} \phi\}$$

$$+ \text{vec}(\phi \phi^T)^H \mathbf{T}_{1,8} \text{vec}(\phi \phi^T)$$

$$\text{s.t. } \phi^H \mathbf{T}_0 \phi - 2\text{Re}\{\mathbf{t}_0^H \phi\} + c_2 - \phi^H \mathbf{T}_{0,0} \phi \quad (20b)$$

$$- 2\text{Re}\{\phi^H \mathbf{T}_{0,5} \phi^* + \text{vec}(\phi \phi^T)^H \mathbf{T}_{0,67} \phi\}$$

$$- \text{vec}(\phi \phi^T)^H \mathbf{T}_{0,8} \text{vec}(\phi \phi^T) \leq 0,$$

$$|\phi_m| = 1, \forall m \in \mathcal{M}. \quad (20c)$$

As seen above, the problem (P2) is highly challenging due to the presence of the quartic and cubic terms in the objective (20a) and the constraint (20b). Note these high-order terms indeed stem from the propagation channel of the radar probing signals, i.e., $\mathbf{H}(\Phi) \triangleq (\mathbf{g}_r + \mathbf{G}_r^H \Phi \mathbf{g}_{RT})(\mathbf{g}_t^H + \mathbf{g}_{RT}^T \Phi \mathbf{G}_t)$, which gives birth to the aforementioned quartic and cubic terms in the SINR functions of the communication and radar sensing signals. To resolve the above difficulty, it is highly desirable that we could somewhat “dissolve” the high-order terms, e.g., reducing the problem from quartic to quadratic, which is much more tractable. In fact, this could be fulfilled via splitting the term Φ in $\mathbf{H}(\Phi)$. Specifically, via introducing a copy Ψ_1 of Φ into $\mathbf{H}(\Phi)$, i.e., we could equivalently rewrite the $\mathbf{H}(\Phi)$ as follows

$$\mathbf{H}(\Phi, \Psi_1) = (\mathbf{g}_r + \mathbf{G}_r^H \Psi_1 \mathbf{g}_{RT})(\mathbf{g}_t^H + \mathbf{g}_{RT}^T \Phi \mathbf{G}_t), \quad (21)$$

where Ψ_1 is indeed a copy of Φ , i.e., $\Phi = \Psi_1$. In fact, via

$$\begin{aligned}
c_{1,0} &\triangleq -\sum_{k=1}^K \{\log(\omega_k) - \omega_k + 1 + 2\text{Re}\{\omega_k \beta_k^* \sqrt{q_k} \mathbf{u}_k^H \mathbf{h}_{BU,k}\} - \omega_k |\beta_k|^2 [\sum_{i=1}^K q_i \mathbf{u}_k^H \mathbf{h}_{BU,i} \mathbf{h}_{BU,i}^H \mathbf{u}_k + \mathbf{v}_k \mathbf{v}_k^H + \sigma_r^2 \|\mathbf{u}_k^H\|_2^2]\}, \quad (19) \\
c_{t,k} &\triangleq \omega_k |\beta_k|^2 \sigma_t, c_{1,1} \triangleq \sum_{k=1}^K c_{t,k} \|\mathbf{a}_{1,k}\|_2^2, c_1 \triangleq c_{1,0} + c_{1,1}, \mathbf{t}_{1,1} \triangleq \sum_{k=1}^K -c_{t,k} (b_{1,k} \mathbf{B}^* \mathbf{a}_{1,k}^*), \mathbf{t}_{1,2} \triangleq \sum_{k=1}^K -c_{t,k} \mathbf{b}_{2,k} \mathbf{a}_{1,k}^H \mathbf{b}_3, \\
\mathbf{t}_{1,0} &\triangleq \sum_{k=1}^K \{\omega_k \beta_k^* \sqrt{q_k} \mathbf{u}_k^H \mathbf{P}_k - \omega_k |\beta_k|^2 [\sum_{i=1}^K q_i (\mathbf{h}_{BU,i}^H \mathbf{u}_k \mathbf{u}_k^H \mathbf{P}_i) + \mathbf{v}_k^H \mathbf{S}_k^*]\}^H, \mathbf{t}_1 \triangleq \mathbf{t}_{1,0} + \mathbf{t}_{1,1} + \mathbf{t}_{1,2}, c_r \triangleq \sigma_r / \Gamma_r, \\
\mathbf{T}_{1,0} &\triangleq \sum_{k=1}^K \{\omega_k |\beta_k|^2 [\sum_{i=1}^K q_i (\mathbf{P}_i^H \mathbf{u}_k \mathbf{u}_k^H \mathbf{P}_i) + \mathbf{S}_k^T \mathbf{S}_k^*]\}, \mathbf{T}_{1,1} \triangleq \sum_{k=1}^K c_{t,k} (|b_{1,k}|^2 \mathbf{B}^* \mathbf{B}^T), \mathbf{T}_{1,2} \triangleq \sum_{k=1}^K c_{t,k} ((\mathbf{B} \mathbf{b}_3)^T \otimes (b_{1,k}^* \mathbf{b}_{2,k})), \\
\mathbf{T}_{1,3} &\triangleq \sum_{k=1}^K c_{t,k} ((\mathbf{b}_3^H \mathbf{B}^H)^T \otimes (b_{1,k} \mathbf{b}_{2,k}^H)), \mathbf{T}_{1,4} \triangleq \sum_{k=1}^K c_{t,k} ((\mathbf{b}_3^H \mathbf{b}_3^H)^T \otimes (\mathbf{b}_{2,k} \mathbf{b}_{2,k}^H)), \mathbf{T}_1 \triangleq \mathbf{T}_{1,0} + \mathbf{T}_{1,1} + \mathbf{T}_{1,2} + \mathbf{T}_{1,3} + \mathbf{T}_{1,4}, \\
\mathbf{T}_{1,5} &\triangleq \sum_{k=1}^K c_{t,k} \mathbf{b}_{2,k} \mathbf{a}_{1,k}^H \mathbf{B}^H, \mathbf{T}_{1,6} \triangleq \sum_{k=1}^K c_{t,k} ((\mathbf{B} \mathbf{B}^H)^T \otimes (b_{1,k}^* \mathbf{b}_{2,k})), \mathbf{T}_{1,7} \triangleq \sum_{k=1}^K c_{t,k} ((\mathbf{b}_3^H \mathbf{B}^H)^T \otimes (\mathbf{b}_{2,k} \mathbf{b}_{2,k}^H)), \\
\mathbf{T}_{1,67} &\triangleq \mathbf{T}_{1,6} + \mathbf{T}_{1,7}, \mathbf{T}_{1,8} \triangleq \sum_{k=1}^K c_{t,k} ((\mathbf{B} \mathbf{B}^H)^T \otimes (\mathbf{b}_{2,k} \mathbf{b}_{2,k}^H)), c_{2,0} \triangleq \sum_{k=1}^K q_k \mathbf{u}_0^H \mathbf{h}_{BU,k} \mathbf{h}_{BU,k}^H \mathbf{u}_0 + \mathbf{v}_0 \mathbf{v}_0^H + \sigma_r^2 \|\mathbf{u}_0^H\|_2^2, \\
c_{2,1} &\triangleq -c_r \|\mathbf{a}_0\|_2^2, c_2 \triangleq c_{2,0} + c_{2,1}, \mathbf{t}_{0,0} \triangleq -(\sum_{k=1}^K q_k (\mathbf{h}_{BU,k}^H \mathbf{u}_0 \mathbf{u}_0^H \mathbf{P}_k) + \mathbf{v}_0^H \mathbf{S}_0^*)^H, \mathbf{t}_{0,1} \triangleq c_r (b_{0,1} \mathbf{B}^* \mathbf{a}_0^*), \mathbf{t}_{0,2} \triangleq c_r (\mathbf{b}_{0,2} \mathbf{a}_0^H \mathbf{b}_3), \\
\mathbf{t}_0 &= \mathbf{t}_{0,0} + \mathbf{t}_{0,1} + \mathbf{t}_{0,2}, \mathbf{T}_0 \triangleq (\sum_{k=1}^K q_k \mathbf{P}_k^H \mathbf{u}_0 \mathbf{u}_0^H \mathbf{P}_k + \mathbf{S}_0^T \mathbf{S}_0^*), \mathbf{T}_{0,1} \triangleq c_r (|b_{0,1}|^2 \mathbf{B}^* \mathbf{B}^T), \mathbf{T}_{0,2} \triangleq c_r (\mathbf{B} \mathbf{b}_3)^T \otimes (\mathbf{b}_{0,2} \mathbf{b}_{0,1}^H), \\
\mathbf{T}_{0,3} &\triangleq c_r (\mathbf{b}_3^H \mathbf{B}^H)^T \otimes (b_{0,1} \mathbf{b}_{0,2}^H), \mathbf{T}_{0,4} \triangleq c_r (\mathbf{b}_3^H \mathbf{b}_3^H)^T \otimes (\mathbf{b}_{0,2} \mathbf{b}_{0,2}^H), \mathbf{T}_{0,0} \triangleq \mathbf{T}_{0,1} + \mathbf{T}_{0,2} + \mathbf{T}_{0,3} + \mathbf{T}_{0,4}, \mathbf{T}_{0,5} \triangleq c_r \mathbf{b}_{0,2} \mathbf{a}_0^H \mathbf{B}^H, \\
\mathbf{T}_{0,6} &\triangleq c_r ((\mathbf{B} \mathbf{B}^H)^T \otimes (b_{0,1}^* \mathbf{b}_{0,2})), \mathbf{T}_{0,7} \triangleq c_r ((\mathbf{b}_3^H \mathbf{B}^H)^T \otimes (\mathbf{b}_{0,2} \mathbf{b}_{0,2}^H)), \mathbf{T}_{0,67} \triangleq \mathbf{T}_{0,6} + \mathbf{T}_{0,7}, \mathbf{T}_{0,8} \triangleq c_r ((\mathbf{B} \mathbf{B}^H)^T \otimes (\mathbf{b}_{0,2} \mathbf{b}_{0,2}^H)).
\end{aligned}$$

introducing the intermediate variable Ψ_1 , optimizing either Φ or Ψ_1 separately with the other one fixed will yield a quadratic problem.

Besides, to decouple the non-convex constant magnitude constraints (20c), we introduce another copy Ψ_2 of Φ , which will yield simple update (as will clear shortly). Based on the discussions, by introducing the two copies Ψ_1 and Ψ_2 of Φ as above, the problem (P2) can be equivalently written as

$$(P3): \min_{\phi, \psi_1, \psi_2} \phi^H (\mathbf{T}_{1,0} + \mathbf{T}_{1,1}) \phi + \psi_1^H \mathbf{T}_{1,2} \psi_1 \quad (22a)$$

$$\begin{aligned}
&+ \phi^H \mathbf{T}_{1,3} \psi_1 + \psi_1^H \mathbf{T}_{1,4} \phi - 2\text{Re}\{(\mathbf{t}_{1,0} + \mathbf{t}_{1,1})^H \phi + \mathbf{t}_{1,2}^H \psi_1\} \\
&+ 2\text{Re}\{\psi_1^H \mathbf{T}_{1,5} \phi^* + \text{vec}(\psi_1 \phi^T)^H (\mathbf{T}_{1,6} \phi + \mathbf{T}_{1,7} \psi_1)\} \\
&+ \text{vec}(\psi_1 \phi^T)^H \mathbf{T}_{1,8} \text{vec}(\psi_1 \phi^T) + c_1
\end{aligned}$$

$$\text{s.t. } \phi^H \mathbf{T}_{0,0} \phi - 2\text{Re}\{(\mathbf{t}_{0,0} + \mathbf{t}_{0,1})^H \phi + \mathbf{t}_{0,2}^H \psi_1\} \quad (22b)$$

$$\begin{aligned}
&- \phi^H \mathbf{T}_{0,1} \phi - \psi_1^H \mathbf{T}_{0,2} \phi - \phi^H \mathbf{T}_{0,3} \psi_1 - \psi_1^H \mathbf{T}_{0,4} \psi_1 \\
&- 2\text{Re}\{\psi_1^H \mathbf{T}_{0,5} \phi^* + \text{vec}(\psi_1 \phi^T)^H (\mathbf{T}_{0,6} \phi + \mathbf{T}_{0,7} \psi_1)\} \\
&- \text{vec}(\psi_1 \phi^T)^H \mathbf{T}_{0,8} \text{vec}(\psi_1 \phi^T) + c_2 \leq 0
\end{aligned}$$

$$\phi = \psi_1, \quad \phi = \psi_2, \quad (22c)$$

$$|\psi_{2,m}| = 1, \forall m \in \mathcal{M}. \quad (22d)$$

To solve the above problem (P3), following the PDD framework [27], we turn to optimize its augmented Lagrangian (AL) problem, given as follows

$$(P4): \min_{\phi, \psi_1, \psi_2, \lambda_1, \lambda_2} \phi^H (\mathbf{T}_{1,0} + \mathbf{T}_{1,1}) \phi + \psi_1^H \mathbf{T}_{1,2} \psi_1 \quad (23a)$$

$$\begin{aligned}
&+ \phi^H \mathbf{T}_{1,3} \psi_1 + \psi_1^H \mathbf{T}_{1,4} \phi - 2\text{Re}\{(\mathbf{t}_{1,0} + \mathbf{t}_{1,1})^H \phi + \mathbf{t}_{1,2}^H \psi_1\} \\
&+ 2\text{Re}\{\psi_1^H \mathbf{T}_{1,5} \phi^* + \text{vec}(\psi_1 \phi^T)^H (\mathbf{T}_{1,6} \phi + \mathbf{T}_{1,7} \psi_1)\} \\
&+ \text{vec}(\psi_1 \phi^T)^H \mathbf{T}_{1,8} \text{vec}(\psi_1 \phi^T) + c_1 \\
&+ \frac{1}{2\rho} \|\phi - \psi_1\|_2^2 + \text{Re}\{\lambda_1^H (\phi - \psi_1)\} \\
&+ \frac{1}{2\rho} \|\phi - \psi_2\|_2^2 + \text{Re}\{\lambda_2^H (\phi - \psi_2)\}
\end{aligned}$$

$$\begin{aligned}
\text{s.t. } &\phi^H \mathbf{T}_{0,0} \phi - 2\text{Re}\{(\mathbf{t}_{0,0} + \mathbf{t}_{0,1})^H \phi + \mathbf{t}_{0,2}^H \psi_1\} \\
&- \phi^H \mathbf{T}_{0,1} \phi - \psi_1^H \mathbf{T}_{0,2} \phi - \phi^H \mathbf{T}_{0,3} \psi_1 - \psi_1^H \mathbf{T}_{0,4} \psi_1
\end{aligned} \quad (23b)$$

$$\begin{aligned}
&- 2\text{Re}\{\psi_1^H \mathbf{T}_{0,5} \phi^* + \text{vec}(\psi_1 \phi^T)^H (\mathbf{T}_{0,6} \phi + \mathbf{T}_{0,7} \psi_1)\} \\
&- \text{vec}(\psi_1 \phi^T)^H \mathbf{T}_{0,8} \text{vec}(\psi_1 \phi^T) + c_2 \leq 0 \\
&|\psi_{2,m}| = 1, \forall m \in \mathcal{M}.
\end{aligned} \quad (23c)$$

Guided by the PDD framework [27], we conduct a two-layer iteration procedure, with its inner layer updating ϕ , ψ_1 and ψ_2 in a block coordinate descent (BCD) manner and its outer layer selectively updating the penalty coefficient ρ or the dual variables $\{\lambda_1, \lambda_2\}$. The PDD procedure will be elaborated in the following.

Inner Layer Procedure

For the inner layer iteration, we will update ϕ , ψ_1 and ψ_2 in sequence. When $\{\psi_1, \psi_2\}$ are given, the minimization of AL with respect to (w.r.t.) ϕ reduces to solving the following problem

$$(P5): \min_{\phi} \phi^H \hat{\mathbf{T}}_1 \phi - 2\text{Re}\{\hat{\mathbf{t}}_1^H \phi\} + \hat{c}_1 \quad (24a)$$

$$\begin{aligned}
&+ \frac{1}{2\rho} \|\phi - \psi_1\|_2^2 + \text{Re}\{\lambda_1^H (\phi - \psi_1)\} \\
&+ \frac{1}{2\rho} \|\phi - \psi_2\|_2^2 + \text{Re}\{\lambda_2^H (\phi - \psi_2)\}
\end{aligned}$$

$$\text{s.t. } \phi^H \mathbf{T}_{0,0} \phi - 2\text{Re}\{\hat{\mathbf{t}}_0^H \phi\} + \hat{c}_2 - \phi^H \mathbf{T}_{0,9} \phi \leq 0, \quad (24b)$$

where the newly introduced coefficients are defined as follows

$$\mathbf{h}_{\psi_1} \triangleq \mathbf{g}_r + \mathbf{G}_r^H \text{diag}(\psi_1) \mathbf{g}_{RT}, \mathbf{G}_{t1} \triangleq \text{diag}(\mathbf{g}_{RT}^T) \mathbf{G}_t, \quad (25)$$

$$\mathbf{t}_{1,3} \triangleq -\sum_{k=1}^K c_{t,k} (\mathbf{G}_{t1}^* \mathbf{W}^* \mathbf{W}^T \mathbf{g}_t^* \mathbf{h}_{\psi_1}^T \mathbf{u}_k^T \mathbf{u}_k^H \mathbf{h}_{\psi_1}^*),$$

$$\mathbf{T}_{1,9} \triangleq \sum_{k=1}^K c_{t,k} ((\mathbf{G}_{t1} \mathbf{W} \mathbf{W}^H \mathbf{G}_{t1}^H)^T \otimes (\mathbf{h}_{\psi_1} \mathbf{u}_k \mathbf{u}_k^H \mathbf{h}_{\psi_1}^H)),$$

$$c_{1,2} \triangleq \sum_{k=1}^K c_{t,k} \|\mathbf{u}_k^H \mathbf{h}_{\psi_1} \mathbf{g}_t^H \mathbf{W}\|_2^2, c_{2,2} \triangleq -c_r \|\mathbf{u}_0^H \mathbf{h}_{\psi_1} \mathbf{g}_t^H \mathbf{W}\|_2^2,$$

$$\mathbf{t}_{0,3} \triangleq c_r (\mathbf{G}_{t1}^* \mathbf{W}^* \mathbf{W}^T \mathbf{g}_t^* \mathbf{h}_{\psi_1}^T \mathbf{u}_0^T \mathbf{u}_0^H \mathbf{h}_{\psi_1}^*),$$

$$\mathbf{T}_{0,9} \triangleq c_r ((\mathbf{G}_{t1} \mathbf{W} \mathbf{W}^H \mathbf{G}_{t1}^H)^T \otimes (\mathbf{h}_{\psi_1} \mathbf{u}_0 \mathbf{u}_0^H \mathbf{h}_{\psi_1}^H)),$$

$$\hat{c}_1 \triangleq c_{1,0} + c_{1,2}, \hat{\mathbf{t}}_1 \triangleq \mathbf{t}_{1,0} + \mathbf{t}_{1,3}, \hat{\mathbf{T}}_1 \triangleq \mathbf{T}_{1,0} + \mathbf{T}_{1,9},$$

$$\hat{c}_2 \triangleq c_{2,0} + c_{2,2}, \hat{\mathbf{t}}_0 \triangleq \mathbf{t}_{0,0} + \mathbf{t}_{0,3}.$$

Obviously, the problem (P5) is non-convex since the constraint (24b) is nonconvex. We adopt the MM framework [28]

to convexify (24b) via taking linearization of convex terms at the point of ϕ_0 , which is given as

$$\phi^H \mathbf{T}_{0,9} \phi \geq 2\text{Re}\{\phi_0^H \mathbf{T}_{0,9}(\phi - \phi_0)\} + \phi_0^H \mathbf{T}_{0,9} \phi_0. \quad (26)$$

Therefore, we turn to replace the term $\phi^H \mathbf{T}_{0,9} \phi$ in constraint (24b) by (26), and the problem (P5) is rewritten as

$$(P6) : \min_{\phi} \phi^H \hat{\mathbf{T}}_1 \phi - 2\text{Re}\{\hat{\mathbf{t}}_1^H \phi\} + \hat{c}_1 \quad (27a)$$

$$+ \frac{1}{2\rho} \|\phi - \psi_1\|_2^2 + \text{Re}\{\boldsymbol{\lambda}_1^H(\phi - \psi_1)\} \\ + \frac{1}{2\rho} \|\phi - \psi_2\|_2^2 + \text{Re}\{\boldsymbol{\lambda}_2^H(\phi - \psi_2)\}$$

$$\text{s.t. } \phi^H \mathbf{T}_{0,0} \phi - 2\text{Re}\{\hat{\mathbf{t}}_0^H \phi\} + \hat{c}_2 \leq 0, \quad (27b)$$

where $\hat{\mathbf{t}}_0 \triangleq \bar{\mathbf{t}}_0 + \mathbf{T}_{0,9}^H \phi_0$ and $\hat{c}_2 \triangleq \bar{c}_2 + (\phi_0^H \mathbf{T}_{0,9} \phi_0)^*$. The problem (P6) is a typical second order cone program (SOCP) and can be solved by existing convex optimization solvers, e.g., CVX [30].

Given the variables $\{\phi, \psi_2\}$, the optimization of updating the auxiliary variable ψ_1 is formulated as

$$(P7) : \min_{\psi_1} \psi_1^H \mathbf{T}_{1,10} \psi_1 - 2\text{Re}\{\mathbf{t}_{1,3}^H \psi_1\} + \tilde{c}_1 \quad (28a)$$

$$+ \frac{1}{2\rho} \|\phi - \psi_1\|_2^2 + \text{Re}\{\boldsymbol{\lambda}_1^H(\phi - \psi_1)\}$$

$$\text{s.t. } -2\text{Re}\{\mathbf{t}_{0,4}^H \psi_1\} + \tilde{c}_2 - \psi_1^H \mathbf{T}_{0,10} \psi_1 \leq 0, \quad (28b)$$

where the above newly introduced coefficients defined as

$$\mathbf{h}_2 \triangleq \mathbf{g}_t + \mathbf{G}_t^H \text{diag}(\phi)^H \mathbf{g}_{RT}^*, \mathbf{G}_{r1} \triangleq \text{diag}(\mathbf{g}_{RT}^H) \mathbf{G}_r, \quad (29)$$

$$c_{1,3} \triangleq \sum_{k=1}^K c_{k,t} \|\mathbf{u}_k^H \mathbf{g}_r \mathbf{h}_2^H \mathbf{W}\|_2^2,$$

$$\mathbf{t}_{1,4} \triangleq -\sum_{k=1}^K c_{k,t} (\mathbf{G}_{r1} \mathbf{u}_k \mathbf{u}_k^H \mathbf{g}_r \mathbf{h}_2^H \mathbf{W} \mathbf{W}^H \mathbf{h}_2),$$

$$\mathbf{T}_{1,10} \triangleq \sum_{k=1}^K c_{k,t} ((\mathbf{h}_2^H \mathbf{W} \mathbf{W}^H \mathbf{h}_2)^T \otimes (\mathbf{G}_{r1} \mathbf{u}_k \mathbf{u}_k^H \mathbf{G}_{r1}^H)),$$

$$c_{2,3} \triangleq -c_r \|\mathbf{u}_0^H \mathbf{g}_r \mathbf{h}_2^H \mathbf{W}\|_2^2,$$

$$\mathbf{t}_{0,4} \triangleq c_r (\mathbf{G}_{r1} \mathbf{u}_0 \mathbf{u}_0^H \mathbf{g}_r \mathbf{h}_2^H \mathbf{W} \mathbf{W}^H \mathbf{h}_2),$$

$$\mathbf{T}_{0,10} \triangleq c_r ((\mathbf{h}_2^H \mathbf{W} \mathbf{W}^H \mathbf{h}_2)^T \otimes (\mathbf{G}_{r1} \mathbf{u}_0 \mathbf{u}_0^H \mathbf{G}_{r1}^H)),$$

$$\tilde{c}_1 \triangleq \phi^H \mathbf{T}_{1,0} \phi - 2\text{Re}\{\mathbf{t}_{1,0}^H \phi\} + c_{1,0} + c_{1,3},$$

$$\tilde{c}_2 \triangleq \phi^H \mathbf{T}_{0,0} \phi - 2\text{Re}\{\mathbf{t}_{0,0}^H \phi\} + c_{2,0} + c_{2,3}.$$

Obviously, the non-convex constraint (28b) makes the problem (P7) intractable. Therefore, still following the MM method, we linearize the quadratic term $\psi_1^H \mathbf{T}_{0,10} \psi_1$ to obtain a tight lower bound as follows

$$\psi_1^H \mathbf{T}_{0,10} \psi_1 \geq 2\text{Re}\{\psi_{1,0}^H \mathbf{T}_{0,10}(\psi_1 - \psi_{1,0})\} + \psi_{1,0}^H \mathbf{T}_{0,10} \psi_{1,0}, \quad (30)$$

where $\psi_{1,0}$ is the value obtained in the last iteration. Therefore, by replace the term $\psi_1^H \mathbf{T}_{0,10} \psi_1$ by (30), the problem (P7) can be rewritten as

$$(P8) : \min_{\psi_1} \psi_1^H \mathbf{T}_{1,10} \psi_1 - 2\text{Re}\{\mathbf{t}_{1,3}^H \psi_1\} + \tilde{c}_1 \quad (31a)$$

$$+ \frac{1}{2\rho} \|\phi - \psi_1\|_2^2 + \text{Re}\{\boldsymbol{\lambda}_1^H(\phi - \psi_1)\}$$

$$\text{s.t. } -2\text{Re}\{\tilde{\mathbf{t}}_{0,4}^H \psi_1\} + \tilde{c}_2 \leq 0, \quad (31b)$$

where $\tilde{\mathbf{t}}_{0,4} \triangleq \mathbf{t}_{0,4} + \mathbf{T}_{0,10}^H \psi_{1,0}$ and $\tilde{c}_2 \triangleq \tilde{c}_2 + (\psi_{1,0}^H \mathbf{T}_{0,10} \psi_{1,0})^*$. The problem (P8) is also an SOCP and solved by CVX.

When $\{\phi, \psi_1\}$ are fixed, the update of the auxiliary variable

ψ_2 is meant to solve

$$(P9) : \min_{\psi_2} \frac{1}{2\rho} \|\phi - \psi_2\|_2^2 + \text{Re}\{\boldsymbol{\lambda}_2^H(\phi - \psi_2)\} \quad (32a)$$

$$\text{s.t. } |\psi_{2,m}| = 1, \forall m \in \mathcal{M}. \quad (32b)$$

Since ψ_2 has unit modulus entries, the quadratic term with respect to ψ_2 in the objective function (32a) is constant, i.e., $\|\psi_2\|_2^2/(2\rho) = M/(2\rho)$. Hence the problem (P9) is reduced to

$$(P10) : \max_{|\psi_2|=1_M} \text{Re}\{(\phi + \rho \boldsymbol{\lambda}_2)^H \psi_2\} \quad (33a)$$

Note that the maximum of problem (P10) can be readily achieved when the elements of ψ_2 are all aligned with those of the linear coefficient $(\rho^{-1} \phi + \boldsymbol{\lambda}_2)$, which is given as

$$\psi_2^* = \exp(j \cdot \angle(\phi + \rho \boldsymbol{\lambda}_2)). \quad (34)$$

Since the inner layer update ϕ, ψ_1 and ψ_2 in a BCD manner, the objective value of (P4) will monotonically converge.

Outer Layer Procedure

When its convergence is reached, we adjust the value of dual variables $\{\boldsymbol{\lambda}_1, \boldsymbol{\lambda}_2\}$ or the penalty coefficient ρ in the outer layer. Specifically,

1) when the equations $\phi = \psi_1$ and $\phi = \psi_2$ are approximately achieved, i.e., $\|\phi - \psi_1\|_\infty$ and $\|\phi - \psi_2\|_\infty$ are simultaneously smaller than some predefined diminishing threshold η_k [27], then the dual variables $\boldsymbol{\lambda}_i$ will be updated in a gradient ascent manner as follows:

$$\boldsymbol{\lambda}_i^{(k+1)} := \boldsymbol{\lambda}_i^{(k)} + \rho^{-1}(\phi - \psi_i), \quad i \in \{1, 2\}; \quad (35)$$

2) when the equality constraints $\phi = \psi_1$ and/or $\phi = \psi_2$ are far from “being true”, in order to force $\phi = \psi_1$ and/or $\phi = \psi_2$ being achieved in the subsequent iterations, the outer layer will increase the penalty parameter ρ^{-1} as follows:

$$(\rho^{(k+1)})^{-1} := c^{-1} \cdot (\rho^{(k)})^{-1}, \quad (36)$$

where c is a predetermined positive constant which is usually smaller than 1 and typically chosen in the range of [0.8, 0.9] [27].

The PDD-based method to solve problem (P2) is summarized in Algorithm 1.

D. Updating The BS Beamformer \mathbf{W}

In this subsection, we discuss the update of the transmit beamformer \mathbf{W} . With other variables being fixed, the optimization problem of updating \mathbf{W} can be formulated as

$$(P11) : \min_{\mathbf{w}} \mathbf{w}^H \mathbf{D}_1 \mathbf{w} - c_3 \quad (37a)$$

$$\text{s.t. } \mathbf{w}^H \mathbf{D}_2 \mathbf{w} - \mathbf{w}^H \mathbf{D}_3 \mathbf{w} + c_4 \leq 0, \quad (37b)$$

$$\mathbf{w}^H \mathbf{w} \leq P_{BS}. \quad (37c)$$

with the new parameters defined as follows

$$\mathbf{w} \triangleq \text{vec}(\mathbf{W}), c_4 \triangleq \left(\sum_{k=1}^K q_k |\mathbf{u}_0^H \mathbf{h}_{U,k}|^2 + \sigma_r^2 \|\mathbf{u}_0^H\|_2^2 \right), \quad (38)$$

$$\mathbf{D}_2 \triangleq \mathbf{I}_{N_t} \otimes \mathbf{G}^H \mathbf{u}_0 \mathbf{u}_0^H \mathbf{G}, \mathbf{D}_3 \triangleq (\mathbf{I}_{N_t} \otimes \sigma_t^2 \mathbf{H}^H \mathbf{u}_0 \mathbf{u}_0^H \mathbf{H}) / \Gamma_r,$$

$$c_3 = \left[\sum_{k=1}^K (\log(\omega_k) - \omega_k + 2\text{Re}\{\omega_k \beta_k^* \sqrt{q_k} \mathbf{u}_k^H \mathbf{h}_{U,k}\} - \omega_k |\beta_k|^2 (\sum_{i=1}^K q_i |\mathbf{u}_k^H \mathbf{h}_{U,i}|^2 + \sigma_r^2 \|\mathbf{u}_k^H\|_2^2) + 1) \right],$$

Algorithm 1 PDD Method to Solve (P2)

```

1: initialize  $\phi^{(0)}, \psi_i^{(0)}, \lambda_i^{(0)}, \rho^{(0)}, i \in \{1, 2\}$  and  $k = 1$ ;
2: repeat
3:   set  $\phi^{(k-1,0)} := \phi^{(k-1)}, \psi_i^{(k-1,0)} := \psi_i^{(k-1)}, t = 0$ ;
4:   repeat
5:     update  $\phi^{(k-1,t+1)}$  by solving (P6);
6:     update  $\psi_1^{(k-1,t+1)}$  by solving (P8);
7:     update  $\psi_2^{(k-1,t+1)}$  by (34);
8:      $t++$ ;
9:   until convergence
10:  set  $\phi^{(k)} := \phi^{(k-1,\infty)}, \psi_i^{(k)} := \psi_i^{(k-1,\infty)}$ ;
11:  if  $\|\phi^{(k)} - \psi_1^{(k)}\|_\infty \leq \eta_k$  and  $\|\phi^{(k)} - \psi_2^{(k)}\|_\infty \leq \eta_k$ 
then
12:     $\lambda_i^{(k+1)} := \lambda_i^{(k)} + \frac{1}{\rho^{(k)}}(\phi^{(k)} - \psi_i^{(k)}), \rho^{(k+1)} := \rho^{(k)}$ ;
13:  else
14:     $\lambda_i^{(k+1)} := \lambda_i^{(k)}, 1/\rho^{(k+1)} := 1/(c \cdot \rho^{(k)})$ ;
15:  end if
16:   $k++$ ;
17: until  $\|\phi^{(k)} - \psi_1^{(k)}\|_2$  and  $\|\phi^{(k)} - \psi_2^{(k)}\|_2$  are sufficiently
small simultaneously;

```

$$\mathbf{D}_1 \triangleq \sum_{k=1}^K \omega_k |\beta_k|^2 (\mathbf{I}_{N_t} \otimes \sigma_t^2 \mathbf{H}^H \mathbf{u}_k \mathbf{u}_k^H \mathbf{H} + \mathbf{I}_{N_t} \otimes \mathbf{G}^H \mathbf{u}_k \mathbf{u}_k^H \mathbf{G}).$$

It can be observed that the problem (P11) is still difficult to solve due to the difference of convex (DC) form constraint (37b). Inspired by the MM framework, we construct a linear lower-bound of the constraint (37b), which is given as

$$\mathbf{w}^H \mathbf{D}_3 \mathbf{w} \geq 2\text{Re}\{\mathbf{w}_0^H \mathbf{D}_3 (\mathbf{w} - \mathbf{w}_0)\} + \mathbf{w}_0^H \mathbf{D}_3 \mathbf{w}_0, \quad (39)$$

where \mathbf{w}_0 is obtained from the last iteration. Therefore, the nonconvex constraint (37b) can be replaced by (39) and the optimization problem (P11) is rewritten as

$$(P12) : \min_{\mathbf{w}} \mathbf{w}^H \mathbf{D}_1 \mathbf{w} - c_3 \quad (40a)$$

$$\text{s.t. } \mathbf{w}^H \mathbf{D}_2 \mathbf{w} - 2\text{Re}\{\mathbf{d}_3^H \mathbf{w}\} + \hat{c}_4 \leq 0, \quad (40b)$$

$$\mathbf{w}^H \mathbf{w} \leq P_{BS}, \quad (40c)$$

where $\mathbf{d}_3 \triangleq \mathbf{D}_3^H \mathbf{w}_0$ and $\hat{c}_4 \triangleq c_4 + (\mathbf{w}_0^H \mathbf{D}_3 \mathbf{w}_0)^*$. The problem (P12) is an SOCP and solved by CVX.

E. Optimizing The User Transmission Power

With other variables being given, the optimization problem of all the users' transmission power $\{q_k\}$ can be formulated as

$$(P13) : \min_{\{q_k\}} \sum_{k=1}^K a_k q_k + \sum_{k=1}^K b_k \sqrt{q_k} - c_5 \quad (41a)$$

$$\text{s.t. } \sum_{k=1}^K d_k q_k \leq \hat{c}_5, \quad (41b)$$

$$0 \leq q_k \leq P_{U,k}, \forall k \in \mathcal{K}, \quad (41c)$$

where the newly introduced coefficients are defined as follows

$$a_k \triangleq \sum_{j=1}^K \omega_j |\beta_j|^2 |\mathbf{u}_j^H \mathbf{h}_{U,k}|^2, d_k \triangleq |\mathbf{u}_0^H \mathbf{h}_{U,k}|^2, \quad (42)$$

$$\hat{c}_5 \triangleq \sigma_t^2 \|\mathbf{u}_0^H \mathbf{H} \mathbf{W}\|_2^2 / \Gamma_r - \|\mathbf{u}_0^H \mathbf{G} \mathbf{W}\|_2^2 - \sigma_r^2 \|\mathbf{u}_0^H\|_2^2,$$

$$b_k \triangleq -2\text{Re}(\omega_k \beta_k^* \mathbf{u}_k^H \mathbf{h}_{U,k}), c_5 \triangleq \sum_{k=1}^K \{\log(\omega_k) - \omega_k$$

$$- \omega_k |\beta_k|^2 (\sigma_t^2 \|\mathbf{u}_k^H \mathbf{H} \mathbf{W}\|_2^2 + \|\mathbf{u}_k^H \mathbf{G} \mathbf{W}\|_2^2 + \sigma_r^2 \|\mathbf{u}_k^H\|) + 1\}.$$

The problem (P13) can still be formulated into an SOCP problem and can be numerically solved.

F. Optimizing The Receiver Filter $\{\mathbf{u}_k\}$

The update of $\{\mathbf{u}_k\}$ are meant to solve the following problem

$$(P14) : \min_{\{\mathbf{u}_k\}} \sum_{k=1}^K (\mathbf{u}_k^H \mathbf{F}_k \mathbf{u}_k - 2\text{Re}\{\mathbf{u}_k^H \tilde{\mathbf{h}}_{U,k}\}) - c_6 \quad (43a)$$

where the above newly introduced coefficients are defined as

$$\tilde{\mathbf{h}}_{U,k} \triangleq \omega_k \beta_k^* \sqrt{q_k} \mathbf{h}_{U,k}, c_6 \triangleq \sum_{k=1}^K (\log(\omega_k) + \omega_k + 1), \quad (44)$$

$$\mathbf{F}_k \triangleq \omega_k |\beta_k|^2 \left(\sum_{i=1}^K q_i \mathbf{h}_{U,i} \mathbf{h}_{U,i}^H + \sigma_t^2 \mathbf{H} \mathbf{W} \mathbf{W}^H \mathbf{H}^H + \mathbf{G} \mathbf{W} \mathbf{W}^H \mathbf{G}^H + \sigma_r^2 \mathbf{I}_{N_r} \right).$$

It is obviously that the problem (P14) can be decomposed into K independent sub-problems, which each subproblem being given as

$$(P15_k) : \min_{\mathbf{u}_k} \mathbf{u}_k^H \mathbf{F}_k \mathbf{u}_k - 2\text{Re}\{\mathbf{u}_k^H \tilde{\mathbf{h}}_{U,k}\} \quad (45a)$$

Notice that the problem (P15_k) is a typical unconstrained convex quadratic problem. Its optimal solution can be easily obtained via setting its derivative to zero and obtained as follows

$$\mathbf{u}_k^* = \mathbf{F}_k^{-1} \tilde{\mathbf{h}}_{U,k}, \forall k \in \mathcal{K}. \quad (46)$$

G. Optimizing The Target Signal Receiver Filter \mathbf{u}_0

After fixing other variables, the optimization problem w.r.t. \mathbf{u}_0 is reduced to a feasibility check problem

$$(P16) : \text{Find } \mathbf{u}_0 \quad (47a)$$

$$\text{s.t. } \mathbf{u}_0^H \mathbf{E}_1 \mathbf{u}_0 - \mathbf{u}_0^H \mathbf{E}_2 \mathbf{u}_0 \leq 0. \quad (47b)$$

where the new parameters in the above are defined as

$$\mathbf{E}_2 \triangleq \sigma_t^2 \mathbf{H} \mathbf{W} \mathbf{W}^H \mathbf{H}^H / \Gamma_r, \quad (48)$$

$$\mathbf{E}_1 \triangleq \left(\sum_{k=1}^K q_k \mathbf{h}_{U,k} \mathbf{h}_{U,k}^H + \mathbf{G} \mathbf{W} \mathbf{W}^H \mathbf{G}^H + \sigma_r^2 \mathbf{I}_{N_r} \right).$$

The feasibility characterization problem (P16), whose objective is missing, is also known as Phase-I problem [39]. To solve it, we consider another closely related problem as follows

$$(P17) : \min_{\mathbf{u}_0, \alpha_u} \alpha_u \quad (49a)$$

$$\text{s.t. } \mathbf{u}_0^H \mathbf{E}_1 \mathbf{u}_0 - \mathbf{u}_0^H \mathbf{E}_2 \mathbf{u}_0 \leq \alpha_u. \quad (49b)$$

To see the connection between (P16) and (P17), suppose that the optimal solution to (P17) is $(\mathbf{u}_0^*, \alpha_u^*)$. If $\alpha_u^* \leq 0$, then α_u^* is actually a feasible solution to (P16). Note that (P17) is assured to have a feasible solution yielding non-positive α_u if the whole iteration starts from a feasible point. Minimizing (P17) is meant to find a more "feasible" \mathbf{u}_0 , which provides a larger margin to satisfy the constraint (47b) and hence benefits the optimization of other variables.

Algorithm 2 Proposed Algorithm to Solve (P1)

```
1: randomly generate feasible  $\phi^{(0)}$ ,  $\mathbf{W}^{(0)}$ ,  $\{q_k^0\}$ ,  $\{\mathbf{u}_k\}$ ,  $\mathbf{u}_0$ ,  
   and  $i = 0$ ;  
2: repeat  
3:   update  $\{\beta_k^{(i+1)}\}$  and  $\{\omega_k^{(i+1)}\}$  by (15) and (16), respec-  
   tively.  
4:   update  $\phi^{(i+1)}$  by invoking Alg.1;  
5:   set  $\mathbf{W}^{(i,0)} := \mathbf{W}^{(i)}$ ,  $m = 0$ ;  
6:   repeat  
7:     update  $\mathbf{W}^{(i,m+1)}$  by solving (P12);  
8:      $m++$ ;  
9:   until convergence;  
10:  set  $\mathbf{W}^{(i+1)} := \mathbf{W}^{(i,\infty)}$ ;  
11:  update  $\{q_k^{(i+1)}\}$  by solving (P13);  
12:  update  $\{\mathbf{u}_k^{(i+1)}\}$  by (46);  
13:  set  $\mathbf{u}_0^{(i,0)} := \mathbf{u}_0^{(i)}$ ,  $m = 0$ ;  
14:  repeat  
15:    update  $\mathbf{u}_0^{(i,m+1)}$  by (53);  
16:     $m++$ ;  
17:  until convergence;  
18:  set  $\mathbf{u}_0^{(i+1)} := \mathbf{u}_0^{(i,\infty)}$ ;  
19:   $i++$ ;  
20: until convergence;
```

Obviously, the problem (P17) obtains optimality only when (49b) achieves equality. Therefore, solving (P17) is equivalent to minimizing the left hand side of (49b), i.e., (50).

$$(P18) : \min_{\mathbf{u}_0} \mathbf{u}_0^H \mathbf{E}_1 \mathbf{u}_0 - \mathbf{u}_0^H \mathbf{E}_2 \mathbf{u}_0 \quad (50)$$

Since the objective function (50) is DC form, we again adopt the MM method to convexify the term $-\mathbf{u}_0^H \mathbf{E}_2 \mathbf{u}_0$ by linearization as follows

$$\begin{aligned} -\mathbf{u}_0^H \mathbf{E}_2 \mathbf{u}_0 &\leq -\hat{\mathbf{u}}_0^H \mathbf{E}_2 \hat{\mathbf{u}}_0 - 2\text{Re}\{\hat{\mathbf{u}}_0^H \mathbf{E}_2 (\mathbf{u}_0 - \hat{\mathbf{u}}_0)\} \\ &= -2\text{Re}\{\hat{\mathbf{u}}_0^H \mathbf{E}_2 \mathbf{u}_0\} + (\hat{\mathbf{u}}_0^H \mathbf{E}_2 \hat{\mathbf{u}}_0)^*, \end{aligned} \quad (51)$$

where $\hat{\mathbf{u}}_0$ is feasible solution obtained in the last iteration.

Therefore, replacing the term $-\mathbf{u}_0^H \mathbf{E}_2 \mathbf{u}_0$ by (51), we turn to optimize a tight convex upper bound of the objective (P18), which is given as

$$(P19) : \min_{\mathbf{u}_0} \mathbf{u}_0^H \mathbf{E}_1 \mathbf{u}_0 - 2\text{Re}\{\hat{\mathbf{u}}_0^H \mathbf{E}_2 \mathbf{u}_0\} + (\hat{\mathbf{u}}_0^H \mathbf{E}_2 \hat{\mathbf{u}}_0)^* \quad (52)$$

The problem (P19) is also a unconstrained convex quadratic problem and its optimal solution can be directly obtained as

$$\mathbf{u}_0^* = \mathbf{E}_1^{-1} (\mathbf{E}_2^H \hat{\mathbf{u}}_0). \quad (53)$$

The overall algorithm to solve problem (P1) is specified in Algorithm 2.

IV. LOW-COMPLEXITY ALGORITHM

Note that our previously proposed Alg.2 relies on numerical solvers, e.g., CVX, to update various block coordinates, including \mathbf{W} , ϕ and $\{q_k\}$. This feature may give rise to some undesirable properties:

i) general convex optimization solvers, including CVX, relies on interior point (IP) method [35] to resolve SOCP

problems, whose complexity increases dramatically when variable's dimension grows.

ii) utilization of third-party solvers inevitably increases cost and inconvenience in implementing the algorithm, e.g., purchase of license, software installation/maintenance and the platform required to support the solver.

Therefore, we proceed to explore solution that, hopefully, does not rely on any numerical solvers.

A. Efficient Update of ϕ

Firstly, in order to efficiently solve (P6) and (P8), we introduce the following lemma that is proved in Appendix A.

Lemma 1. Consider the following problem:

$$(P_{Lm1}) : \min_{\mathbf{x}} \mathbf{x}^H \mathbf{Q} \mathbf{x} - 2\text{Re}\{\mathbf{q}^H \mathbf{x}\} + q \quad (54a)$$

$$\text{s.t. } \mathbf{x}^H \bar{\mathbf{Q}} \mathbf{x} - 2\text{Re}\{\bar{\mathbf{q}}^H \mathbf{x}\} + \bar{q} \leq 0, \quad (54b)$$

where $\mathbf{Q} \succ 0$ and $\bar{\mathbf{Q}} \succcurlyeq 0$, and Slater's condition holds. Then the optimal solution to problem (P_{Lm1}) is given by one of the following two cases:

CASE-I: If $(\mathbf{Q}^{-1} \mathbf{q})^H \bar{\mathbf{Q}} (\mathbf{Q}^{-1} \mathbf{q}) - 2\text{Re}\{\bar{\mathbf{q}}^H (\mathbf{Q}^{-1} \mathbf{q})\} + \bar{q} \leq 0$, then the optimal solution $\mathbf{x}^* = \mathbf{Q}^{-1} \mathbf{q}$.

CASE-II: Otherwise, $\mathbf{x}^* = (\zeta^* \bar{\mathbf{Q}} + \mathbf{Q})^{-1} (\zeta^* \bar{\mathbf{q}} + \mathbf{q})$, where the positive ζ^* is the solution to the following equation

$$\begin{aligned} &((\zeta^* \bar{\mathbf{Q}} + \mathbf{Q})^{-1} (\zeta^* \bar{\mathbf{q}} + \mathbf{q}))^H \bar{\mathbf{Q}} (\zeta^* \bar{\mathbf{Q}} + \mathbf{Q})^{-1} (\zeta^* \bar{\mathbf{q}} + \mathbf{q}) \\ &- 2\text{Re}\{\bar{\mathbf{q}}^H (\zeta^* \bar{\mathbf{Q}} + \mathbf{Q})^{-1} (\zeta^* \bar{\mathbf{q}} + \mathbf{q})\} + \bar{q} = 0. \end{aligned} \quad (55)$$

Note that the value of ζ^* can be efficiently obtained by the Newton's method.

Based on the above Lemma 1, we examine the solution of (P6), which is a preliminary step in PDD procedure. For ease of notations, we denote

$$\mathbf{T}_{1,11} \triangleq \hat{\mathbf{T}}_1 + \mathbf{I}/\rho, \mathbf{t}_{1,4} \triangleq \hat{\mathbf{t}}_1 + \frac{\psi_1 + \psi_2}{2\rho} - \frac{\lambda_1 + \lambda_2}{2}, \quad (56)$$

$$c_{1,4} \triangleq \hat{c}_1 + \frac{\|\psi_1\|_2^2 + \|\psi_2\|_2^2}{2\rho} - \text{Re}\{\lambda_1^H \psi_1 + \lambda_2^H \psi_2\}.$$

Then we can rewrite the problem (P6) as

$$(P20) : \min_{\phi} \phi^H \mathbf{T}_{1,11} \phi - 2\text{Re}\{\mathbf{t}_{1,4}^H \phi\} + c_{1,4} \quad (57a)$$

$$\text{s.t. } \phi^H \mathbf{T}_{0,0} \phi - 2\text{Re}\{\hat{\mathbf{t}}_0^H \phi\} + \hat{c}_2 \leq 0. \quad (57b)$$

Obviously, (P20) can be efficiently solved by Lemma 1.

Next, we turn to obtain the solution of (P8) via Lemma 1. For simplicity, we introduce the new definitions

$$\mathbf{T}_{1,12} \triangleq \mathbf{T}_{1,10} + \mathbf{I}/2\rho, \mathbf{t}_{1,5} \triangleq \mathbf{t}_{1,3} + \frac{\phi}{2\rho} + \frac{\lambda_1}{2}, \quad (58)$$

$$c_{1,5} \triangleq \tilde{c}_1 + \frac{\|\phi\|_2^2}{2\rho} + \text{Re}\{\lambda_1^H \phi\}.$$

The problem (P8) can be equivalently rewritten as

$$(P21) : \min_{\psi_1} \psi_1^H \mathbf{T}_{1,12} \psi_1 - 2\text{Re}\{\mathbf{t}_{1,5}^H \psi_1\} + c_{1,5} \quad (59a)$$

$$\text{s.t. } -2\text{Re}\{\hat{\mathbf{t}}_{0,4}^H \psi_1\} + \hat{c}_2 \leq 0. \quad (59b)$$

It is obvious that the above problem (P21) also can be easily solved by Lemma 1.

B. Efficient Update of \mathbf{w}

In this subsection, we investigate low complexity solution to the problem (P12) in Sec. III-B. Firstly, to develop analytic solution, we introduce an auxiliary variable \mathbf{f} and transform (P12) into an equivalent form as follows

$$(P22) : \min_{\mathbf{w}, \mathbf{f}} \mathbf{w}^H \mathbf{D}_1 \mathbf{w} - c_3 \quad (60a)$$

$$\text{s.t. } \mathbf{f}^H \mathbf{D}_2 \mathbf{f} - 2\text{Re}\{\mathbf{d}_3^H \mathbf{f}\} + \hat{c}_4 \leq 0, \quad (60b)$$

$$\mathbf{w}^H \mathbf{w} \leq P_{BS}, \quad (60c)$$

$$\mathbf{w} = \mathbf{f}. \quad (60d)$$

We then proceed via adopting the ADMM methodology [29] to solve the above problem. Specifically, by penalizing the equality constraint (60d) in the objective, the AL problem of (P22) is given as

$$(P23) : \min_{\mathbf{w}, \mathbf{f}, \boldsymbol{\tau}} \mathbf{w}^H \mathbf{D}_1 \mathbf{w} + \text{Re}\{\boldsymbol{\tau}^H (\mathbf{w} - \mathbf{f})\} + \frac{\nu}{2} \|\mathbf{w} - \mathbf{f}\|_2^2 \quad (61a)$$

$$\text{s.t. } \mathbf{f}^H \mathbf{D}_2 \mathbf{f} - 2\text{Re}\{\mathbf{d}_3^H \mathbf{f}\} + \hat{c}_4 \leq 0, \quad (61b)$$

$$\mathbf{w}^H \mathbf{w} \leq P_{BS}, \quad (61c)$$

where ν is a positive constant and $\boldsymbol{\tau} \in \mathbb{C}^{N_t \cdot N_t \times 1}$ is the introduced Lagrangian multiplier associated with (60d). According to the ADMM method, to solve (P23), we alternatively update \mathbf{w} , \mathbf{f} and $\boldsymbol{\tau}$, as specified in the sequel.

With \mathbf{w} and $\boldsymbol{\tau}$ being fixed, the optimization of (P23) w.r.t. \mathbf{f} is given as the following problem

$$(P24) : \min_{\mathbf{f}} \|\mathbf{f}\|_2^2 - 2\text{Re}\{\mathbf{d}_1^H \mathbf{f}\} \quad (62a)$$

$$\text{s.t. } \mathbf{f}^H \mathbf{D}_2 \mathbf{f} - 2\text{Re}\{\mathbf{d}_3^H \mathbf{f}\} + \hat{c}_4 \leq 0, \quad (62b)$$

where $\mathbf{d}_1 \triangleq \boldsymbol{\tau} / \nu + \mathbf{w}$. It is readily seen that (P24) also satisfies the assumptions of Lemma 1 and hence can be easily solved by the results therein. Details are omitted to avoid repetition.

When \mathbf{f} and $\boldsymbol{\tau}$ are given, the update of \mathbf{w} is reduced to solving the following problem

$$(P25) : \min_{\mathbf{w}} \mathbf{w}^H \bar{\mathbf{D}}_1 \mathbf{w} - 2\text{Re}\{\bar{\mathbf{d}}_1^H \mathbf{w}\} \quad (63a)$$

$$\text{s.t. } \mathbf{w}^H \mathbf{w} \leq P_{BS}. \quad (63b)$$

where $\bar{\mathbf{D}}_1 \triangleq \mathbf{D}_1 + \frac{\nu}{2} \mathbf{I}_{N_t \cdot N_t}$ and $\bar{\mathbf{d}}_1 \triangleq \frac{1}{2}(\nu \mathbf{f} - \boldsymbol{\tau})$. Obviously, the problem (P25) can also be efficiently solved by exploiting Lemma 1.

Specifically, the two CASEs identified in Lemma 1 can be accommodated to (P25) as follows

CASE-I: When $(\bar{\mathbf{D}}_1^{-1} \bar{\mathbf{d}}_1)^H (\bar{\mathbf{D}}_1^{-1} \bar{\mathbf{d}}_1) \leq P_0$, the optimal solution $\mathbf{w}^* = \bar{\mathbf{D}}_1^{-1} \bar{\mathbf{d}}_1$.

CASE-II: Otherwise, $\mathbf{w}^* = (\bar{\mathbf{D}}_1 + \kappa^* \mathbf{I}_{N_t \cdot N_t})^{-1} \bar{\mathbf{d}}_1$. The optimal value of κ^* can be efficiently obtained (e.g., Newton's method or bisection search).

Following the ADMM method [29], after the primal variables being updated, the dual variable $\boldsymbol{\tau}$ is updated in a gradient ascent manner, which is given as

$$\boldsymbol{\tau}^{(t+1)} := \boldsymbol{\tau}^{(t)} + \nu(\mathbf{w} - \mathbf{f}). \quad (64)$$

The ADMM-based low complexity method to solve problem (P22), i.e., (P12), is summarized in Algorithm 3.

Algorithm 3 ADMM Method to Solve (P22), i.e., (P12)

- 1: initialize $\mathbf{f}^{(0)}$, $\mathbf{w}^{(0)}$, $\boldsymbol{\tau}^{(0)}$ and $t = 0$;
 - 2: **repeat**
 - 3: update $\mathbf{f}^{(t+1)}$ by solving (P24);
 - 4: update $\mathbf{w}^{(t+1)}$ by solving (P25);
 - 5: update $\boldsymbol{\tau}^{(t+1)}$ by (64);
 - 6: $t++$;
 - 7: **until** convergence;
-

C. Efficient Update of $\{q_k\}$

In this subsection, we develop closed-form solution to update $\{q_k\}$. Firstly, we define $p_k = \sqrt{q_k}$ and $\bar{P}_{U,k} = \sqrt{P_{U,k}}$, and then the problem can be rewritten as

$$(P26) : \min_{\{p_k\}} \sum_{k=1}^K a_k p_k^2 + \sum_{k=1}^K b_k p_k - c_5 \quad (65a)$$

$$\text{s.t. } \sum_{k=1}^K d_k p_k^2 \leq \hat{c}_5, \quad (65b)$$

$$0 \leq p_k \leq \bar{P}_{U,k}, \forall k \in \mathcal{K}. \quad (65c)$$

The above problem indeed has analytic solution as presented in the following theorem, which is proved in Appendix B.

Theorem 1. We define $\hat{p}_k = \min\{-\frac{b_k}{2a_k}, \bar{P}_{U,k}\}$, $\forall k \in \mathcal{K}$. The optimal values of $\{p_k\}$ are obtained according to one of the following two cases:

CASE-I: if $\sum_{k=1}^K d_k \hat{p}_k^2 \leq \hat{c}_5$, the optimal solutions $p_k^* = \hat{p}_k$, $\forall k \in \mathcal{K}$.

CASE-II: Otherwise, the optimal values of $\{p_k\}$ are given as

$$p_k^*(\nu^*) = \left[-\frac{b_k}{2a_k + 2\nu^* d_k} \right]^{\bar{P}_{U,k}}, \forall k \in \mathcal{K}, \quad (66)$$

where $[a]^{\bar{P}} \triangleq \min\{a, \bar{P}\}$, and ν^* is the unique solution to the following equation

$$\sum_{k=1}^K d_k (p_k^*(\nu^*))^2 = \hat{c}_5. \quad (67)$$

The optimal value of ν^* in CASE-II of Theorem 1 can be efficiently obtained by a bisection search procedure. However, the upper-bound of ν^* is still missing. Therefore, the following lemma provides an upper-bound of ν^* , which is proved in Appendix C

Lemma 2. Firstly, we assume that $\{\tilde{p}_k\}$ is any strictly feasible solution of problem (P26) and $\text{obj}(\{\tilde{p}_k\})$ is the objective value of problem (P26) yielded by $\{\tilde{p}_k\}$. Then, following the definition of $\{\hat{p}_k\}$ introduced in Theorem 1, an upper-bound of ν^* is given as

$$\nu^* \leq \frac{\text{obj}(\{\tilde{p}_k\}) - \text{obj}(\{\hat{p}_k\})}{\hat{c}_4 - \sum_{k=1}^K d_k \tilde{p}_k^2}. \quad (68)$$

D. Complexity

In the following, we will discuss the complexity of our proposed algorithms. According to the complexity analysis in [37], for the PDD-based algorithm, the complexity of solving (P2) is $C_4 C_3 (C_1 + C_2) M^3$, where C_1 and C_2 denote the

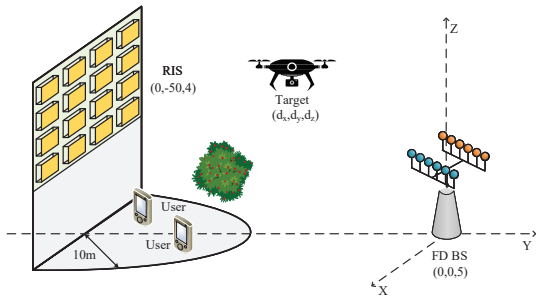


Fig. 2. The experiment scenario model.

iteration number of solving (P6) and (P8) by MM method, respectively. C_3 and C_4 represent the iteration number of the outer and inner PDD loops, respectively. In the each iteration, the complexity of solving SOCP problems (P12) and (P13) are $\mathcal{O}(C_5 N_t^6)$ and $\mathcal{O}(K^3)$, respectively, where C_5 is the number of iterations of solving problem (P12) by the MM method. Therefore, the total computational complexity of Algorithm 2 is approximately given as $\mathcal{O}(C_6(C_4 C_3(C_1 + C_2)M^3 + C_5 N_t^6 + K^3))$ with C_6 represented as the number of iterations to solve problem (P2).

V. NUMERICAL RESULTS

In this section, numerical results are presented to verify our proposals. The setting of the experiment is shown in Fig. 2, where one FD BS tries to detect one target and simultaneously serves 4 users covered by a nearby RIS device. In the experiment, the BS and the RIS are located at the three dimensional (3D) coordinates (0,0,5m) and (0,-50m,4m), respectively. The target is randomly distributed at $(d_x m, d_y m, d_z m)$, where $d_x \in [-1, 1]$, $d_y \in [10, 40]$ and $d_z \in [7, 10]$. All users are randomly distributed within a right half circle of the radius of 10m centered at the RIS at an altitude of 1.5m. The large-scale fading is modeled as $PL = C_0(d/d_0)^{-\alpha}$, where C_0 represents the path loss of the reference distance $d_0 = 1m$, d and α denote the propagation distance and the fading exponent, respectively. The BS TX-RIS/BS RX-RIS links and self-interference link follow Rician distribution with Rician factor of 3dB and 5dB, respectively. The BS TX-user links and RIS-user links all are assumed to be independent and identically distributed Rayleigh fading channels. The BS TX-target, BS RX-target and RIS-target links are modeled as line-of-sight (LoS) channels. The path loss exponents of BS TX-User, BS TX-RIS, BS RX-RIS, RIS-User, RIS-target, BS TX-target and BS RX-target are $\alpha_{BU} = 3.6$, $\alpha_{BTR} = \alpha_{BRR} = 2.7$, $\alpha_{RU} = 2.4$, $\alpha_{RT} = 2.2$ and $\alpha_{BT} = \alpha_{TB} = 2.2$, respectively. The path loss of both self-interference channels is $\rho_{SI} = -110$ dB due to the self-interference cancellation [38]. In addition, the numbers of BS transmit antennas N_t vary from 2 to 14 and the number of RIS elements M ranges from 50 to 1000. In most tests, $N_t = N_r = 4$ and $M = 100$ if not specially stated. The transmit power for the BS is set as 30dBm. The noise power and the predefined target detection level of BS are set as $\sigma_{BS}^2 = -90$ dBm and $\Gamma_r = 5$ dB, respectively. The RCS is $\sigma_t^2 = 1$.

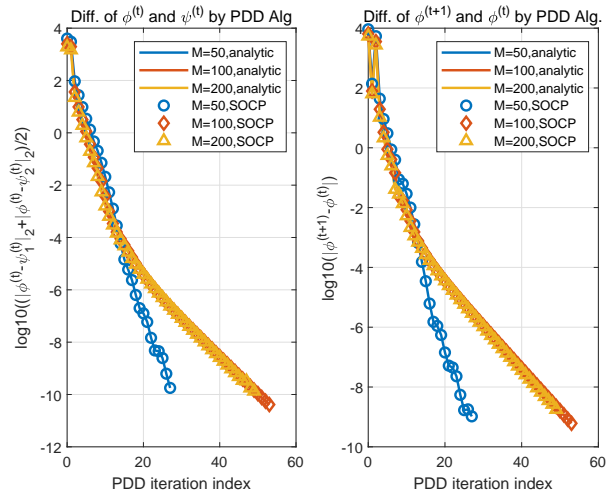


Fig. 3. Convergence of PDD method optimizing ϕ (Alg.1).

TABLE I: MATLAB Run Time to Update ϕ

Method	$M=50$	$M=100$	$M=200$	$M=500$	$M=1000$
SOCP	0.3689	0.3864	0.4910	0.5066	0.8145
analytic	0.0001	0.0004	0.0014	0.0082	0.0444

Firstly, Fig. 3 illustrates the converge behaviour of our proposed SOCP-based and analytic-based PDD methods updating the RIS phase-shifts ϕ . For fair comparison, both the SOCP and KKT implementations start from one common initial point. In Fig. 3, under various settings of number of RIS elements M , the left and right subfigure demonstrate the difference $|\phi^{(t)} - \psi^{(t)}|_2$ and $|\phi^{(t+1)} - \phi^{(t)}|_2$ in log domain, respectively, along with the progress of PDD iterations. As reflected by Fig. 3, both the SOCP-based and the analytic-based yields nearly identical performance. The PDD method generally converges well within 60 iterations, i.e., the discrepancy between ϕ and ψ , the variation in ϕ itself is below 10^{-6} . However, it is worth noting that the analytic-based solution has much lower complexity than the SOCP counterpart (see the following comments for Table I&II).

Next, in Table I&II, we examine the complexity of our proposed analytic-based PDD solution. To this end, we compare the MATLAB runtime of the SOCP-based and the analytic-based methods under different settings of M . Recall that these two competing methods have identical performance as demonstrated in Fig. 3. As shown in Table I&II, our proposed analytic solutions are highly efficient. In fact, the run time of the analytic-based solution is generally one or two orders of magnitude smaller than that of the SOCP one.

In Fig. 4 and Fig. 5, we examine the convergence of the analytic-based solution Alg. 3 to optimize \mathbf{W} using ADMM framework. Note when solving (P24) and (P25), we rescale their objective and constraint to set the maximal eigenvalue of quadratic coefficient as 1. Based on that, different values of coefficient ν are tested. The left and right half of Fig. 4 represents the value of $|\mathbf{f}^{(t+1)} - \mathbf{f}^{(t)}|_2^2$ and $|\mathbf{f}^{(t)} - \mathbf{w}^{(t)}|_2^2$ in log domain, respectively. According to Fig. 4, an appropriate value of the penalty coefficient ν can be chosen in the range of

TABLE II: MATLAB Run Time to Update ψ_1

Method	$M=50$	$M=100$	$M=200$	$M=500$	$M=1000$
SOCP	0.3144	0.3242	0.3321	0.3515	0.3684
analytic	0.0001	0.0004	0.0013	0.0081	0.0447

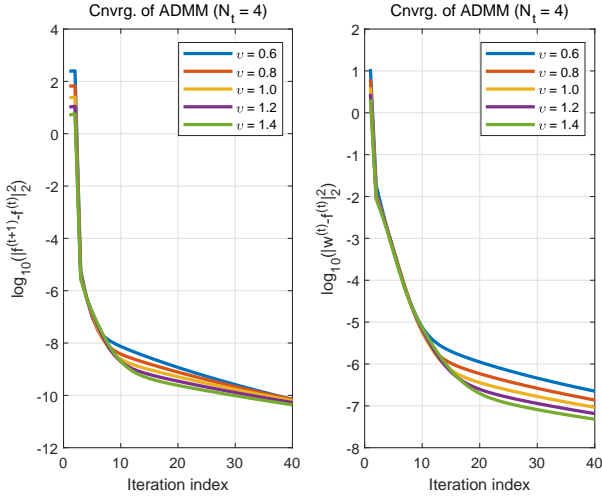


Fig. 4. Convergence of ADMM method.

[0.6,1.4], which yields sufficient convergence (e.g., precision of 10^{-6}) within several tens of iterations.

Fig. 5 examines the objective convergence yielded by Alg. 3. The left subfigure presents the objective value iterates. The true objective value of (P11) obtained via utilizing SOCP solver (i.e., CVX) is also presented as a benchmark, which is normalized. The right half of Fig. 5 represents the difference between the true objective value and that yielded by Alg. 3 in log domain. Generally, Alg. 3 yields sufficiently accurate objective value within 10 iterations.

In Table III, we examine the complexity of the analytic-based solution Alg. 3. Under different settings of the BS antenna numbers N_t , the MATLAB runtime of CVX and Alg. 3 are presented in the table. As shown by the results, the Alg. 3's runtime is smaller than one or two orders of magnitude of that of the SOCP solver.

In Fig. 6, we check the overall convergence behaviours of our proposed algorithms to tackle the original problem (P1), including both the SOCP-based and low-complexity (Low com.) solutions. In all tests, the SOCP-based and analytic-based solutions both start from identical initial points. As seen from the figure, both algorithms exhibit identical performance and generally converge within 10 iterations.

In Fig. 7, we illustrate the sum-rate versus the number of RIS units. For comparison, we consider the without RIS ("noRIS") and random phase-shift RIS ("rndRIS") schemes and the HD system. It is clearly observe that by increasing the number of RIS' units, the schemes assisted by RIS all monotonically increase the sum-rate. Moreover, our proposed algorithm significant outperforms both "noRIS" and "rndRIS" schemes in FD and HD systems, respectively. Besides, we can see that the sum-rate of the FD system is larger than that of the HD system in all schemes.

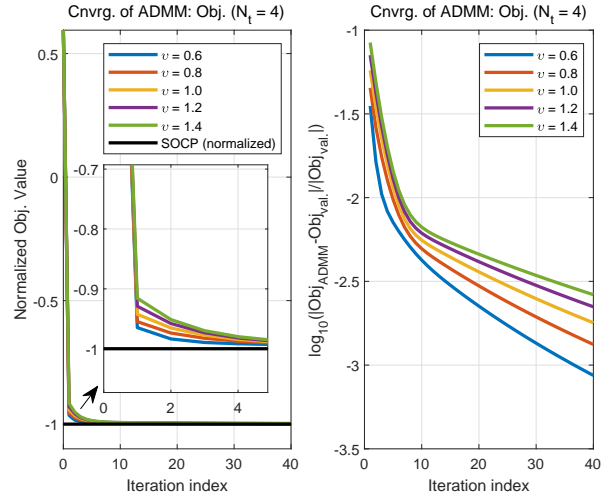


Fig. 5. Convergence of objective value of ADMM method.

 TABLE III: MATLAB Run Time to Update \mathbf{W}

Alg.	$N_t=2$	$N_t=4$	$N_t=8$	$N_t=12$	$N_t=14$
SOCP	0.3139	0.3173	0.3324	0.3632	0.4319
ADMM	0.0034	0.0053	0.0319	0.1152	0.1894

In Fig. 8, we examine the impact of the magnitude of SI channel. The horizontal axis represents the SI coefficient ρ_{SI} , which is proportional to the magnitude of SI channel \mathbf{H}_s [38]. As can be seen, sum-rate drops when SI increases. Compared to the no-RIS scenario, the deployment of RIS significantly boosts the sum-rate.

Fig. 9 demonstrates the achievable sum-rate versus the predefined target detection level Γ_r . It is observed that the sum-rate of all users decreases as Γ_r increases, which reveals the trade-off between the performance of communication and radar sensing. In addition, the $M = 100$ case can achieve better performance than the $M = 50$ case.

VI. CONCLUSIONS

This paper investigates the joint active and passive beamforming design problem in an RIS aided FD ISAC system that performs target sensing and UL communication functionality simultaneously. We propose an iterative solution to jointly design RIS configuration, users' power allocation and receiving processors to achieve both radar sensing and communication functionals. Besides, we further develop a fully analytic based solution, which does not depend on any numerical solvers and has low complexity. Numerical results demonstrate the efficiency and effectiveness of our proposed algorithms and manifest the benefit of deploying RIS in the uplink FD ISAC system.

APPENDIX

A. Proof of Lemma 1

Proof: According to the hypothesis, strongly duality holds for the problem (P_{Lm1}) and it has unique solution since its objective is strictly convex. We identify (P_{Lm1})'s optimal solution via checking its Karush-Kuhn-Tucker (KKT) conditions

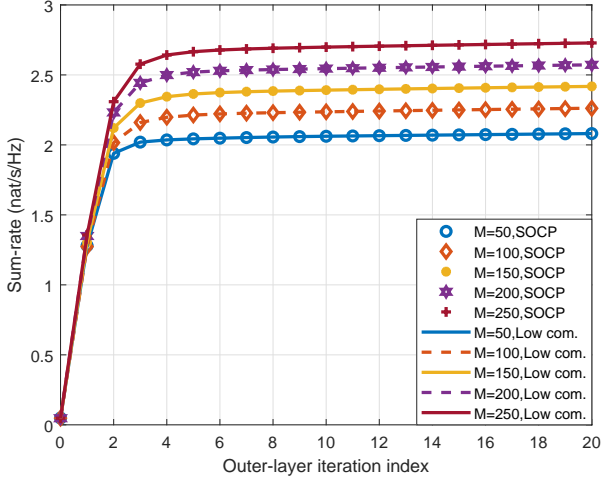


Fig. 6. Convergence of Alg. 2.

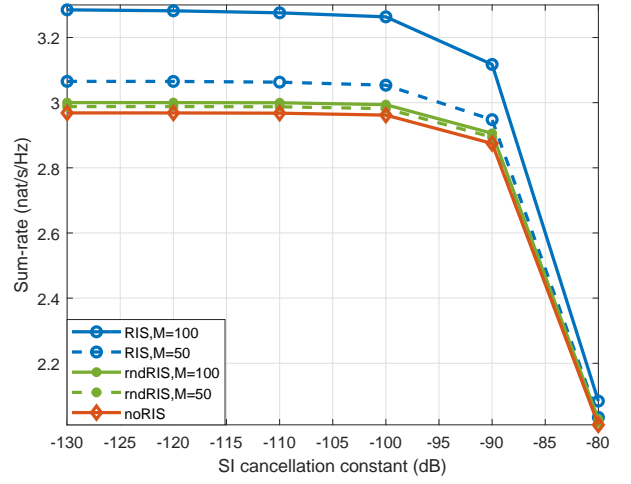


Fig. 8. The impact of SI channel.

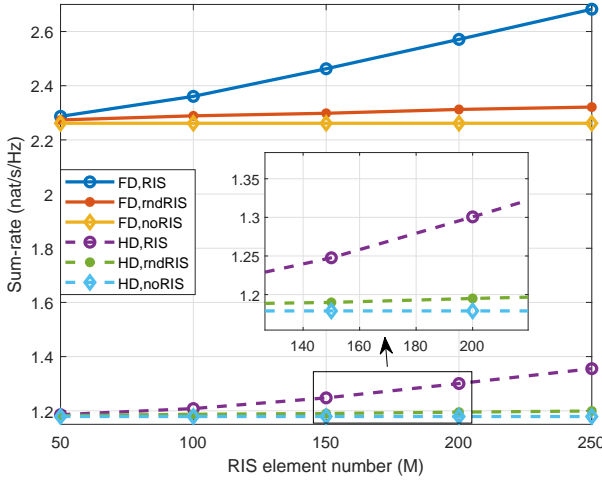


Fig. 7. The impact of RIS on communication rate.

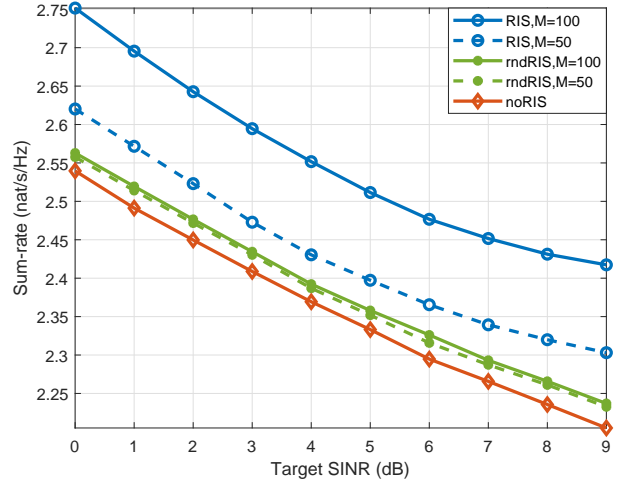


Fig. 9. Sum-rate versus Γ_r .

[39]. Denote the Lagrangian multiplier associated with the constraint of (P_{Lm1}) as ς . Then the KKT conditions of (P_{Lm1}) are given as

$$\varsigma \geq 0, \mathbf{x}^H \bar{\mathbf{Q}} \mathbf{x} - 2\text{Re}\{\bar{\mathbf{q}}^H \mathbf{x}\} + \bar{q} \leq 0, \quad (69a)$$

$$\varsigma(\mathbf{x}^H \bar{\mathbf{Q}} \mathbf{x} - 2\text{Re}\{\bar{\mathbf{q}}^H \mathbf{x}\} + \bar{q}) = 0, \quad (69b)$$

$$\mathbf{Q} \mathbf{x} - \mathbf{q} + \varsigma(\bar{\mathbf{Q}} \mathbf{x} - \bar{\mathbf{q}}) = 0. \quad (69c)$$

Since the ς is non-negative, we consider two possible cases according to the sign of ς as follows

CASE-I: if $\varsigma^* = 0$, by (69c), we can directly obtain

$$\mathbf{x}^* = \mathbf{Q}^{-1} \mathbf{q}. \quad (70)$$

At this point, the KKT conditions (69) will be satisfied if and only if the inequality $(\mathbf{x}^*)^H \bar{\mathbf{Q}} \mathbf{x}^* - 2\text{Re}\{\bar{\mathbf{q}}^H \mathbf{x}^*\} + \bar{q} \leq 0$ is satisfied. If this inequality stands true, then \mathbf{x}^* in (70) is indeed the optimal solution. Otherwise, (69) cannot be satisfied and it implies that ς^* should be positive, as discussed in the following case.

CASE-II: When $\varsigma^* > 0$, by (69b) and (69c) we have

$$\mathbf{x}^* = (\varsigma^* \bar{\mathbf{Q}} + \mathbf{Q})^{-1} (\varsigma^* \bar{\mathbf{q}} + \mathbf{q}). \quad (71)$$

Since $(\mathbf{Q}^{-1} \mathbf{q})^H \bar{\mathbf{Q}} (\mathbf{Q}^{-1} \mathbf{q}) - 2\text{Re}\{\bar{\mathbf{q}}^H (\mathbf{Q}^{-1} \mathbf{q})\} + \bar{q} > 0$, hence there have a unique positive ς^* satisfying

$$\begin{aligned} & ((\varsigma^* \bar{\mathbf{Q}} + \mathbf{Q})^{-1} (\varsigma^* \bar{\mathbf{q}} + \mathbf{q}))^H \bar{\mathbf{Q}} (\varsigma^* \bar{\mathbf{Q}} + \mathbf{Q})^{-1} (\varsigma^* \bar{\mathbf{q}} + \mathbf{q}) \\ & - 2\text{Re}\{\bar{\mathbf{q}}^H (\varsigma^* \bar{\mathbf{Q}} + \mathbf{Q})^{-1} (\varsigma^* \bar{\mathbf{q}} + \mathbf{q})\} + \bar{q} = 0. \end{aligned} \quad (72)$$

The unique ς^* can be obtained by the Newton's method. Therefore, Lemma 1 has been proved.

B. Proof of Theorem 1

Proof: Firstly, one critical observation is that we can just assume that $b_k < 0$ for all $k \in \mathcal{K}$ without loss of optimality. In fact, if $b_k \geq 0$ for some specific k , then obviously $p_k^* = 0$ minimizes the summand associated with p_k in the objective while not affecting the power allocation to other users as constrained in (65b).

Next, we consider to determine the optimal solutions of (P26) when $b_k < 0, \forall k \in \mathcal{K}$. Obviously, Slater's condition for (P26) when all p_k 's take sufficiently small positive values. Therefore, strong duality holds for (P26) and we determine its optimal value via analyzing its KKT conditions.

Via introducing the Lagrangian multipliers $\{\eta_k\}, \{\gamma_k\}$ and ν associated with the constraints of (P26), $0 \leq p_k, p_k \leq \bar{P}_{U,k}$ and $\sum_{k=1}^K d_k p_k^2 \leq \hat{c}_5$, respectively, the KKT conditions are given as

$$0 \leq p_k \leq \bar{P}_{U,k}, \gamma_k \geq 0, \eta_k \geq 0, \nu \geq 0, \sum_{k=1}^K d_k p_k^2 - \hat{c}_5 \leq 0, \quad (73a)$$

$$\gamma_k(p_k - \bar{P}_{U,k}) = 0, \eta_k p_k = 0, \nu(\sum_{k=1}^K d_k p_k^2 - \hat{c}_5) = 0, \quad (73b)$$

$$2a_k p_k + b_k + \gamma_k - \eta_k + 2\nu d_k p_k = 0, \forall k \in \mathcal{K}. \quad (73c)$$

In the following, we will analyze the KKT conditions in two possible cases according to the sign value of ν , i.e., $\nu = 0$ or $\nu > 0$.

CASE-I: $\nu^* = 0$. Via (73a), we can have $\sum_{k=1}^K d_k p_k^{*2} \leq \hat{c}_5$. Then we investigate the value of γ_k .

case-i: if $\gamma_k^* > 0$, by (73b), we immediately have $p_k^* = \bar{P}_{U,k}$ and hence $\eta_k^* = 0$. Therefore, (73c) is equivalently rewritten as

$$\gamma_k^* = -(2a_k \bar{P}_{U,k} + b_k) > 0. \quad (74)$$

Since $\gamma_k^* > 0$, $\bar{P}_{U,k}$ need to satisfy $\bar{P}_{U,k} < (-b_k)/(2a_k)$. Otherwise, γ_k^* will not be positive and then this sub-case can not occur.

case-ii: if $\gamma_k^* = 0$, via (73b), we have $0 \leq p_k^* \leq \bar{P}_{U,k}$ and $\eta_k^* \geq 0$. The equation (73c) is transformed into

$$\gamma_k^* = -2a_k p_k^* - b_k + \eta_k^* = 0, \forall k \in \mathcal{K}. \quad (75)$$

Then, we will obtain

$$p_k^* = (\eta_k^* - b_k)/(2a_k), \quad (76)$$

$$\eta_k^* = 2a_k p_k^* + b_k. \quad (77)$$

Since p_k^* lies in the range $[0, \bar{P}_{U,k}]$, η_k^* also has a bounded range $[b_k, 2a_k \bar{P}_{U,k} + b_k]$. Since $\eta_k^* \geq 0$, this is possible only if the upper-bound $2a_k \bar{P}_{U,k} + b_k \geq 0$, i.e., $(-b_k)/(2a_k) \leq \bar{P}_{U,k}$. Otherwise, case-ii could not occur.

Besides, we notice that $\eta_k^* = 0$. In fact, if $\eta_k^* > 0$, then $p_k^* = 0$ and hence (77) implies $\eta_k^* = b_k$. Since $b_k < 0$ as previously discussed, the equality $\eta_k^* = b_k$ cannot stand. Therefore, $\eta_k^* = 0$ and the optimal solution $p_k^* = (-b_k)/(2a_k)$.

Summarizing the above two sub-cases, we readily obtain

$$\gamma_k^* = [-(2a_k \bar{P}_{U,k} + b_k)]^+, \quad (78a)$$

$$p_k^* = \min\{\bar{P}_{U,k}, (-b_k)/(2a_k)\}, \forall k \in \mathcal{K}, \quad (78b)$$

where $[x]^+ \triangleq \max\{x, 0\}$. Note that (78b) will satisfy all KKT conditions in (73a)-(73c) except for the sum-power constraint $\sum_{k=1}^K d_k p_k^{*2} \leq \hat{c}_5$. If this constraint is satisfied, the value of $\{p_k\}$ in (78b) is the optimal solution to problem (P26). However, if $\sum_{k=1}^K d_k p_k^{*2} > \hat{c}_5$, CASE-I would not occur, and then we further to consider CASE-II, i.e., $\nu > 0$.

CASE-II: $\nu^* > 0$. By (73b), we have $\sum_{k=1}^K d_k p_k^{*2} = \hat{c}_5$.

Similar to CASE-I, we also consider two possible subcases of γ_k in the following.

case-i: If $\gamma_k^* > 0$, then by (73b), we have $p_k^* = \bar{P}_{U,k}$ and $\eta_k^* = 0$. The equation (73c) is reduced to

$$\gamma_k^* + 2a_k \bar{P}_{U,k} + b_k + 2\nu^* d_k \bar{P}_{U,k} = 0, \quad (79)$$

which is equivalent to

$$\gamma_k^* = -2a_k \bar{P}_{U,k} - b_k - 2\nu^* d_k \bar{P}_{U,k}. \quad (80)$$

Since $\gamma_k^* > 0$ by assumption, this requires

$$\nu^* < -\frac{a_k}{d_k} - \frac{b_k}{2d_k \bar{P}_{U,k}}. \quad (81)$$

Therefore, associated with $\nu^* > 0$, the following condition

$$0 < \nu^* < -\frac{a_k}{d_k} - \frac{b_k}{2d_k \bar{P}_{U,k}} \quad (82)$$

should be satisfied. Otherwise, case-i could not occur.

case-ii: If $\gamma_k^* = 0$, via (73b) we have $0 < p_k^* \leq \bar{P}_{U,k}$ and $\eta_k^* \geq 0$. Therefore, by (73c), we obtain

$$p_k^* = \frac{\eta_k^* - b_k}{2a_k + 2\nu^* d_k}, \quad (83)$$

$$\eta_k^* = 2a_k p_k^* + b_k + 2\nu^* d_k p_k^*. \quad (84)$$

Since p_k^* has a range of $[0, \bar{P}_{U,k}]$, η_k^* takes value in the range $[b_k, 2(a_k + \nu^* d_k) \bar{P}_{U,k} + b_k]$. Due to $\eta_k^* \geq 0$, the upper-bound of η_k^* should satisfy $2(a_k + \nu^* d_k) \bar{P}_{U,k} + b_k \geq 0$. Therefore, the ν^* can only take value in the range as follows

$$\nu^* \geq -\frac{a_k}{d_k} - \frac{b_k}{2d_k \bar{P}_{U,k}}. \quad (85)$$

Following similar arguments as in CASE-I, it can be shown that $\eta_k^* = 0$. Therefore, $\eta_k^* = 0$ holds and the optimal solution p_k^* is given as

$$p_k^* = -\frac{b_k}{2a_k + 2\nu^* d_k}. \quad (86)$$

If $\nu^* < -\frac{a_k}{d_k} - \frac{b_k}{2d_k \bar{P}_{U,k}}$, η_k^* will be negative and this sub-case could not occur indeed. Summarizing the above two sub-cases and comparing the conditions in (82) and (85), we have the optimal solution as follows

$$p_k^*(\nu^*) = \left[-\frac{b_k}{2a_k + 2\nu^* d_k} \right]_{\bar{P}_{U,k}}. \quad (87)$$

Note that $p_k^*(\nu^*)$ is a monotonically decreasing function in ν^* and $p_k^*(0) = \min\{-\frac{b_k}{2a_k}, \bar{P}_{U,k}\} = \hat{p}_k^*$. Therefore, when ν^* decreases $+\infty$ to 0, the value of $p_k^*(\nu^*)$ varies 0 to \hat{p}_k^* . According to $\sum_{k=1}^K d_k \hat{p}_k^{*2} > \hat{c}_5$ in CASE-II, hence there exists an unique positive ν^* satisfying $\sum_{k=1}^K d_k (p_k^*(\nu^*))^2 = \hat{c}_5$.

C. Proof of Lemma 3

Proof: Consider the following optimization problem

$$(P27) : \min_{\{p_k\}} \sum_{k=1}^K a_k p_k^2 + \sum_{k=1}^K b_k p_k \quad (88a)$$

$$\text{s.t. } 0 \leq p_k \leq \bar{P}_{U,k}, \forall k \in \mathcal{K}, \quad (88b)$$

where the problem (P27) is a relaxation of (P26) by ignoring the sun-power constraint (65b).

According to the definition of $\{\hat{p}_k\}$ given in Theorem 1, it is easily to prove that $\{\hat{p}_k\}$ is indeed the optimal solution of (P27). Hence, we have $\text{obj}(\{p_k^*\}) \geq \text{obj}(\{\hat{p}_k\})$.

Next, the problem (P26) is rewritten in an equivalent form as follows:

$$(P28) : \min_{\mathcal{Q}} \sum_{k=1}^K a_k p_k^2 + \sum_{k=1}^K b_k p_k \quad (89a)$$

$$\text{s.t.} \sum_{k=1}^K d_k p_k^2 \leq \hat{c}_4, \quad (89b)$$

where we define the convex set \mathcal{Q} as $\mathcal{Q} \triangleq \{\{p_k\} | 0 \leq p_k \leq \bar{P}_{U,k}, \forall k \in \mathcal{K}\}$. The Lagrangian of (P28) is formulated as

$$\mathcal{L}(\{p_k\}, \nu) = \sum_{k=1}^K a_k p_k^2 + \sum_{k=1}^K b_k p_k + \nu (\sum_{k=1}^K d_k p_k^2 - \hat{c}_4). \quad (90)$$

Since the Slater's condition of problem (P28) is obviously satisfied, and then strong duality holds. Therefore, we can obtain a saddle point of the Lagrangian in (P28) [39] via a pair of optimal primal-dual variables $(\{p_k^*\}, \nu^*)$. Then we have the following relations

$$\text{obj}(\{\hat{p}_k\}) \leq \text{obj}(\{p_k^*\}) = \mathcal{L}(\{p_k^*\}, \nu^*) \quad (91)$$

$$\stackrel{(a)}{=} \min_{\{p_k\} \in \mathcal{Q}} \left\{ \sum_{k=1}^K a_k p_k^2 + \sum_{k=1}^K b_k p_k + \nu^* (\sum_{k=1}^K d_k p_k^2 - \hat{c}_5) \right\}$$

$$\stackrel{(b)}{\leq} \sum_{k=1}^K a_k \tilde{p}_k^2 + \sum_{k=1}^K b_k \tilde{p}_k + \nu^* (\sum_{k=1}^K d_k \tilde{p}_k^2 - \hat{c}_5),$$

where (a) is due to the saddle point theorem [39] and (b) holds because $\{\tilde{p}_k\}$ is an arbitrary strictly feasible solution to problem (P26). Note that $\sum_{k=1}^K d_k \tilde{p}_k^2 < \hat{c}_5$ is satisfied according to the choice of $\{\tilde{p}_k\}$. Lastly, we rearrange the equality (91) and then obtain the upper-bound in (68).

REFERENCES

- [1] F. Liu, C. Masouros, A. P. Petropulu, H. Griffiths, and L. Hanzo, "Joint radar and communication design: Applications, state-of-the-art, and the road ahead," *IEEE Trans. Commun.*, vol. 68, no. 6, pp. 3834-3862, Jun. 2020.
- [2] F. Liu *et al.*, "Integrated sensing and communications: Toward dual-functional wireless networks for 6G and beyond," *IEEE J. Sel. Areas Commun.*, vol. 40, no. 6, pp. 1728-1767, Jun. 2022.
- [3] J. A. Zhang *et al.*, "Enabling joint communication and radar sensing in mobile networks: a survey," *IEEE Commun. Surveys & Tutorials*, vol. 24, no. 1, pp. 306-345, Firstquarter 2022.
- [4] C. Pan *et al.*, "An overview of signal processing techniques for RIS/IRS-aided wireless systems," *IEEE J. Sel. Topics Signal Process.*, vol. 16, no. 5, pp. 883-917, Aug. 2022.
- [5] Q. Wu, S. Zhang, B. Zheng, C. You, and R. Zhang, "Intelligent reflecting surface-aided wireless communications: A tutorial," *IEEE Trans. Commun.*, vol. 69, no. 5, pp. 3313-3351, May 2021.
- [6] X. Wang, Z. Fei, J. Huang, and H. Yu, "Joint waveform and discrete phase shift design for RIS-assisted integrated sensing and communication system under Cramér-Rao bound constraint," *IEEE Trans. Veh. Technol.*, vol. 71, no. 1, pp. 1004-1009, Jan. 2022.
- [7] X. Wang, Z. Fei, Z. Zheng, and J. Guo, "Joint waveform design and passive beamforming for RIS-assisted dual-functional radar-communication system," *IEEE Trans. Veh. Technol.*, vol. 70, no. 5, pp. 5131-5136, May 2021.
- [8] Z.-M. Jiang *et al.*, "Intelligent reflecting surface aided dual-function radar and communication system," *IEEE Syst. J.*, vol. 16, no. 1, pp. 475-486, Mar. 2022.
- [9] S. Yan, S. Cai, W. Xia, J. Zhang, and S. Xia, "A reconfigurable intelligent surface aided dual-function radar and communication system," in *Proc. IEEE Int. Symp. Joint Commun. Sensing (JC&S)*, Seefeld, Austria, Mar. 2022, pp. 1-6.
- [10] Y. Li and A. Petropulu, "Dual-function radar-communication system aided by intelligent reflecting surfaces," in *Proc. 12th IEEE Sensor Array and Multichannel Signal Process. Workshop (SAM)*, Trondheim, Norway, 2022, pp. 430-434.
- [11] M. Hua, Q. Wu, C. He, S. Ma, and W. Chen, "Joint active and passive beamforming design for IRS-aided radar-communication," *IEEE Trans. Wireless Commun.*, vol. 22, no. 4, pp. 2278-2294, Apr. 2023.
- [12] Z. Xing, R. Wang, and X. Yuan, "Passive beamforming design for reconfigurable intelligent surface enabled integrated sensing and communication," Jun. 2022. [Online]. Available: <https://arxiv.org/abs/2206.00525>
- [13] Y. Li and A. Petropulu, "Minorization-based low-complexity design for IRS-aided ISAC systems," in *Proc. 2023 IEEE Radar Conf. (Radar-Conf23)*, San Antonio, TX, USA, 2023, pp. 1-6.
- [14] Y. Xu, Y. Li, J. A. Zhang, and M. D. Renzo, "Joint beamforming for RIS-assisted integrated sensing and communication systems," Mar. 2023. [Online]. Available: <https://arxiv.org/abs/2303.01771>
- [15] Z. Liu, H. Zhang, T. Huang, F. Xu, and Y. C. Eldar, "Hybrid RIS-assisted MIMO dual-function radar-communication system," Mar. 2023. [Online]. Available: <https://arxiv.org/abs/2303.16278>
- [16] Z. Wang, X. Mu, and Y. Liu, "STARS enabled integrated sensing and communications," *IEEE Trans. Wireless Commun.*, early access, February 22, 2023, doi: 10.1109/TWC.2023.3245297.
- [17] Z. Yu, G. Zhou, H. Ren, C. Pan, B. Wang, M. Dong, and J. Wang, "Active RIS aided integrated sensing and communication systems," Feb. 2023. [Online]. Available: <https://arxiv.org/abs/2302.08934>
- [18] K. V. Mishra, A. Chattopadhyay, S. S. Acharjee, and A. P. Petropulu, "Optm3sec: Optimizing multicast IRS-aided multiantenna DFRC secrecy channel with multiple eavesdroppers," in *Proc. IEEE Inter. Conf. Acoust., Speech Signal Process. (ICASSP)*, Singapore, Singapore, Apr. 2022, pp. 9037-9041.
- [19] M. Hua, Q. Wu, W. Chen, O. A. Dobre, and A. L. Swindlehurst, "Secure intelligent reflecting surface aided integrated sensing and communication," *IEEE Trans. Wireless Commun.*, early access, June 02, 2023, doi: 10.1109/TWC.2023.3280179.
- [20] Y. Li and A. Petropulu, "Efficient beamforming designs for IRS-aided DFRC systems," May 2023. [Online]. Available: <https://arxiv.org/abs/2305.06461>
- [21] J. Zuo, Y. Liu, C. Zhu, Y. Zou, D. Zhang, and N. Al-Dhahir, "Exploiting NOMA and RIS in integrated sensing and communication," *IEEE Trans. Veh. Technol.*, early access, May 09, 2023, doi: 10.1109/TVT.2023.3272036.
- [22] L. Wang, L. F. Abanto-Leon, and A. Asadi, "Joint communication and sensing in RIS-enabled mmWave networks," Oct. 2022. [Online]. Available: <https://arxiv.org/abs/2210.03685>
- [23] M. A. Islam, G. C. Alexandropoulos, and B. Smida, "Simultaneous multi-User MIMO communications and multi-target tracking with full duplex radios," in *Proc IEEE Globecom Workshops (GC Wkshps)*, Rio de Janeiro, Brazil, 2022, pp. 19-24.
- [24] Z. Xiao and Y. Zeng, "Waveform design and performance analysis for full-duplex integrated sensing and communication," *IEEE J. Sel. Areas Commun.*, vol. 40, no. 6, pp. 1823-1837, Jun. 2022.
- [25] X. Wang, Z. Fei, J. A. Zhang, and J. Huang, "Sensing-assisted secure uplink communications with full-duplex base station," *IEEE Commun. Lett.*, vol. 26, no. 2, pp. 249-253, Feb. 2022.
- [26] 3GPP Tech. Spec. 38.211, "NR: Physical Channels and Modulation v. 2.0.0"; <http://www.3gpp.org/dynareport/38211.html>
- [27] Q. Shi and M. Hong, "Penalty dual decomposition method for non-smooth nonconvex optimization-part i: Algorithms and convergence analysis," *IEEE Trans. Signal Process.*, vol. 68, pp. 4108-4122, Jun. 2020.
- [28] Y. Sun, P. Babu, and D. P. Palomar, "Majorization-minimization algorithms in signal processing, communications, and machine learning," *IEEE Trans. Signal Process.*, vol. 65, no. 3, pp. 794-816, Feb. 2017.
- [29] S. Boyd, N. Parikh, E. Chu, B. Peleato, and J. Eckstein, "Distributed optimization and statistical learning via the alternating direction method of multipliers," in *Found. and Trends in Machine Learning*, vol. 3, no. 1, pp. 1-122, 2011.
- [30] M. Grant and S. Boyd, *CVX: Matlab software for disciplined convex programming*, version 2.1, <http://cvxr.com/cvx>, Mar. 2014.
- [31] X. Liu, T. Huang, N. Shlezinger, Y. Liu, J. Zhou, and Y. C. Eldar, "Joint transmit beamforming for multiuser MIMO communications and MIMO radar," *IEEE Trans. Signal Process.*, vol. 68, pp. 3929-3944, 2020.
- [32] F. Liu, Y. -F. Liu, A. Li, C. Masouros, and Y. C. Eldar, "Cramér-rao bound optimization for joint radar-communication beamforming," *IEEE Trans. Signal Process.*, vol. 70, pp. 240-253, 2022.
- [33] Q. Shi, M. Razaviyayn, Z. -Q. Luo, and C. He, "An iteratively weighted MMSE approach to distributed sum-utility maximization for a MIMO interfering broadcast channel," *IEEE Trans. Signal Process.*, vol. 59, no. 9, pp. 4331-4340, Sept. 2011.
- [34] D. P. Bertsekas, "Nonlinear programming," *Journal of the Operational Research Society*, vol. 48, no. 3, pp. 334-334, 1997.

- [35] S. Boyd and L. Vandenberghe, *Convex Optimization*. New York: Cambridge University Press, 2004.
- [36] Y. Liu and J. Li, "Linear precoding to optimize throughput, power consumption and energy efficiency in MIMO wireless sensor networks," *IEEE Trans. Commun.*, vol. 66, no. 5, pp. 2122-2136, 2018.
- [37] A. Ben-Tal and A. Nemirovski, "Lectures on Modern Convex Optimization, Analysis, Algorithms, and Engineering Applications." *Society for Industrial and Applied Mathematics (SIAM)*, 2001.
- [38] Y. Sun, D. W. K. Ng, Z. Ding, and R. Schober, "Optimal joint power and subcarrier allocation for full-duplex multicarrier non-orthogonal multiple access systems," *IEEE Trans. Commun.*, vol. 65, no. 3, pp. 1077-1091, Mar. 2017.
- [39] S. Boyd and L. Vandenberghe, *Convex Optimization*. New York: Cambridge University Press, 2004.

